Range Anxiety

Panle Jia Barwick Shanjun Li Tianli Xia *

September 3, 2025

PRELIMINARY: NOT FOR DISTRIBUTION

Abstract

Range anxiety, the fear of depleting battery before reaching a charging station, is often cited as a major barrier to electric vehicle (EV) adoption, yet there has been limited formal economic analysis to quantify its importance and understand the policy implications. We develop a continuous-time dynamic model of EV usage and charging decisions to quantify range anxiety as the utility loss from feasible yet unrealized trips due to perceived range constraints. Using high-frequency data of 188,000 EV trips and 30,000 charging events among 8,000 EVs in Shanghai, we recover model parameters governing consumer driving and charging decisions. The estimates imply that, across EV models with varying driving ranges, average range anxiety was about $1,900 in 2021 but declined to $1,200 in 2024, driven by improvements in charging infrastructure and, especially, increases in driving range. Policy simulations underscore the importance of coordinating investments in battery capacity and charging infrastructure to address range anxiety: relative to socially optimal levels, Shanghai's EV market has under-invested in driving range while over-investing in charging infrastructure.

Keywords: Electric vehicles, range anxiety, charging infrastructure, dynamic model

JEL Classification Codes: L91, R13, R21

*Barwick: Department of Economics, UW-Madison, NBER, and CEPR, pbarwick@wisc.edu. Li: Doerr School of Sustainability and FSI, Stanford University and NBER, shanli@stanford.edu. Xia: Simon Business School, University of Rochester, tianli.xia@rochester.edu. We thank Xiufang Cao for excellent research assistance.

1 Introduction

The transportation sector accounts for about one-third of the global carbon emissions, making its electrification with a clean electricity grid a key strategy for decarbonization. Since being introduced into the mass market in 2011, global passenger EV sales have grown rapidly, reaching 17.1 million units, or 20% of new passenger vehicle sales, by 2024.[1] Market penetration, however, varies widely: EVs accounted for 40% of new vehicle sales in China, 28% in Europe, 11% in the United States, and just 5% in the rest of the world. Even within countries or regions, adoption is highly uneven.[2] Understanding the barriers to EV adoption and identifying solutions to address them is critical for the next phase of EV diffusion.

Consumer surveys and industry reports regularly identify range anxiety as one of the most significant barriers to EV adoption (Wardlaw, 2020; Chokshi et al., 2021; Klier and Rubenstein, 2022; Rainieri et al., 2023; Bloomberg Intelligence, 2024). Range anxiety refers to the fear of depleting the battery before reaching a charging station, stemming from the combination of limited driving range and inadequate charging infrastructure.[3] Despite its widely recognized importance, there is limited economic analysis of range anxiety or of cost-effective strategies to mitigate it. To address this gap in the literature, we develop a micro-foundation of range anxiety using a continuous-time dynamic model of consumer driving and charging decisions. Based on estimated model parameters, we conduct policy simulations to evaluate the relative cost-effectiveness of investing in battery technologies and expanding charging infrastructure.

In the model, trip demands of varying distances arrive exogenously, and EV drivers decide whether to undertake a trip or initiate charging based on their remaining battery range, the convenience of the charging network, and charging prices. We define range anxiety as the utility loss from forgone trips, arising from the driver's perceived risk of having insufficient battery range to reach either the destination or a charging station. Our empirical analysis leverages a unique granular and high-frequency dataset on EV driving and charging behavior. It records the location and remaining range of 8,000 EVs at 5-second intervals, along with detailed information on charging, such as station location, price, charging duration, and quantity. The data contains about 188,000 trips and 30,000 charging events across four weeks

[1] EVs include both battery electric vehicles (BEVs) and plug-in hybrid electric vehicles (PHEVs).

[2] Within Europe, EVs accounted for nearly 90% of new vehicle sales in Norway, compared to less than 20% in Germany. In the U.S., EVs made up about 26% of new car registrations in California in 2024, but less than 7% in Texas.

[3] Early EV models typically offered only 100–200 miles per charge, well below the 300–400 miles that gasoline vehicles can travel on a full tank. In 2015, there were about 12,000 public EV charging stations in the U.S., compared to nearly 150,000 gasoline stations. By 2025, the number of public charging stations had grown to nearly 70,000.

each in 2021 and 2024. Using these rich data, we recover the model parameters to quantify the significance of range anxiety and conduct policy simulations.

We begin by documenting five key patterns in the data. First, the charging probability, defined as the share of charging events among both driving and charging events, is higher when the remaining range (i.e., state of charge) is low. This is intuitive, as a limited remaining range both constrains the ability to take trips and increases the need to recharge. Second, charging probability rises with charging access, especially at low remaining ranges, reflecting the reduced hassle cost when more stations are nearby. Third, charging probability falls with charging price, again most strongly when the remaining range is low. By contrast, when the remaining range is high, charging probability is unresponsive to either charging access or charging price. Fourth, drivers forgo over 60% of trips that would reduce their remaining range below 50 km and about 20% of trips that would leave them below 100 km. The fraction of feasible yet forgone trips declines as the remaining range increases. Assuming that trips arrive independently of the remaining range, these forgone trips provide direct evidence of range anxiety. Fifth, among drivers with access to home chargers, the probability of charging at public stations is much flatter with respect to the remaining range, highlighting behavioral differences between those with and without home charging access.

We then estimate a continuous-time dynamic model to recover the structural parameters governing driving and charging decisions. We incorporate rich heterogeneity and a number of state variables: consumers are characterized by the full driving range of their EV (e.g., 250km vs. 400km), the convenience of their local charging network (dense vs. sparse), and whether they have access to a home charger. We also allow charging prices to vary. The estimates suggest that the probability of charging decreases with remaining range and charging prices, but increases with better charging access, longer driving range, and denser charging networks. In contrast, the probability of driving rises with remaining range but drops sharply when a trip would reduce the remaining range below 50 or 100 km, and especially when a trip would end in areas with sparse or costly charging options. Finally, the estimated price elasticity of charging demand at fast public stations is -0.98 for drivers without home charging and -0.90 for those with home charging.

The model allows us to estimate consumers' willingness to pay (WTP) for driving range and charging access, and the magnitudes are substantial. For drivers without home chargers, the estimated WTP for the improved driving range and charging network between 2018 (average range of 318km and a total of 100 stations in Shanghai) and 2024 (383km and 2,268 stations) is ¥62,000 (or $8,600). For those with access to home chargers, the corresponding WTP is

only ¥18,000 (or $2,500). Interestingly, the WTP for both driving range and charging access exhibits diminishing returns. The estimates also illustrate that driving range and charging access are substitutes: the combined WTP from increasing both attributes is smaller than the sum of their individual contributions.

We next quantify range anxiety by monetizing the utility loss from feasible but unrealized trips due to fear of getting stranded on the road. The estimates suggest that average range anxiety across vehicles with different ranges was $2,550 in 2018, falling to $1,900 in 2021 and $1,200 in 2024. This decline reflects both the expansion of the charging network (from 100 stations in 2018 to 400 in 2021 and 2,268 in 2024) and, especially, improvements in driving range (from 318km in 2018 to 353km in 2021 and 383km in 2024). Overall, the reduction in range anxiety accounts for roughly 15% of WTP for improved driving range and charging access among consumers with home chargers, and over 50% among those without home charging.

We conduct simulations to evaluate two approaches to alleviating range anxiety: improving charging access through denser station networks and increasing driving range via greater battery capacity. The socially optimal levels of both are derived by maximizing aggregated welfare, which is consumer WTP minus the cost of enhancing range and charging access. Our simulations show that the observed levels of charging access and driving range in Shanghai's EV market are markedly different from the social optimum. Driving ranges consistently fell short of the socially optimal levels between 2018 and 2024. Charging infrastructure, by contrast, was undersupplied in 2018 and 2021 but expanded so rapidly that by 2024, the number of stations was twice the social optimum. These findings underscore the importance of coordinating investments in charging networks and battery capacity, especially since both are often supported by government policies such as subsidies.

Our paper contributes to three strands of literature. First, it extends the extensive work on consumer demand for EVs. Prior studies have primarily examined barriers to EV adoption—such as high upfront purchase costs, limited access to charging infrastructure, and the role of government policies in addressing these challenges (Springel, 2021a; Rapson and Muehlegger, 2023). A key finding in this literature is the importance of indirect network effects (the "chicken-and-egg" problem), whereby charging infrastructure investment and EV adoption reinforce each other through positive spillovers (Li et al., 2017; Li, 2023; Springel, 2021b; Jacqz and Johnston, 2024; Wang, 2024). While range anxiety is often invoked as an implicit mechanism linking charging access to EV adoption, it has not, to our knowledge, been formally defined. Qin and Scott (2023) examines the effect of vehicle driving range on EV demand.

In contrast, our paper offers a micro-foundation for range anxiety through a continuous-time dynamic model and quantifies it directly using detailed data on driving and charging behavior.

Second, our paper contributes to the emerging literature on EV charging. A central question in this literature is how charging behavior responds to prices across different settings, including home, workplace, and public stations. Field experiments document substantial variation in price elasticities across contexts (Garg et al., 2024; La Nauze et al., 2024; Bernard et al., 2025; Bailey et al., 2025).[4] Relying on highly disaggregated data, other studies infer EV usage from household electricity consumption in California (Burlig et al., 2021), estimate the time cost of fueling gasoline vehicles among drivers in Michigan and use this estimate to benchmark the cost of charging (Dorsey et al., 2025), and examine the impact of charging on the electricity grid in Germany (Heid et al., 2024). Our paper extends this literature by examining how driving and charging respond to both charging prices and charging access, within a unified framework applied to highly granular observational data. Our structural estimates indicate a price elasticity of –1 for public charging. Notably, EV drivers with home charging exhibit a stronger response to price changes at home than to prices at public stations.

Third, our study contributes to the literature on policy design aimed at promoting EV adoption and infrastructure investment by quantifying the interaction between driving range and charging access through a micro-founded model of EV driving and charging decisions. Zhou and Li (2018) highlight the critical role of indirect network effects in EV diffusion and argue that government intervention may be necessary to coordinate consumer adoption and infrastructure development. Barwick et al. (2024) and Remmy (2025) examine automakers' incentives in supplying product attributes such as driving range, showing that market power and network effects can lead to socially suboptimal outcomes. Relatedly, Arkolakis et al. (2025) and Barwick et al. (2025) develop models to characterize optimal charging networks that account for road network and driving patterns. Complementing these studies, our analysis demonstrates that the combination of limited driving range (supplied by automakers) and sparse charging access (provided by station investors) is the fundamental source of range anxiety, and that this interaction jointly determines the socially optimal levels of vehicle range and charging network size. Our policy simulations further underscore the need to coordinate policy instruments such as subsidies that target different market participants, echoing the insight from Liu (2025) on coordinated policy mix in the EV sector.

[4]For example, interventions on charging prices yield elasticity estimates of –0.4 for workplace charging at UCSD (Garg et al., 2024), –0.44 for home charging among Tesla owners in Australia (La Nauze et al., 2024), and –1.6 for home charging in Calgary (Bailey et al., 2025). A UK national intervention at public charging stations finds price elasticities of -2 to -2.9 (Bernard et al., 2025), with considerable heterogeneity.

The remainder of the paper proceeds as follows. Section 2 describes the data and discusses key data patterns. Section 3 presents the empirical model and estimation strategy. Section 4 discuss the estimation results. Section 5 conducts policy simulations. Section 6 concludes.

2 Data Description

Our analysis draws on data from Shanghai, a city of 24.9 million residents and 4.15 million households. By the end of 2024, approximately 5.1 million passenger vehicles were registered in the city, including 1.51 million electric vehicles (EVs), the highest EV stock of any single city in the world. In 2024 alone, 278,000 new EVs were sold in Shanghai, accounting for 45% of all new passenger vehicle sales in the city, slightly exceeding the national average EV market share of 40%.[5]

Our main dataset consists of eight weekly cross-sections of detailed EV usage and driving data, with four weeks drawn from 2021 and four from 2024. The four weeks fall in January, March, August, and October to represent the four seasons. Each cross-section includes 1,100 battery EVs with information on all the trips and charging events of each EV during the week. The EVs in the sample were randomly chosen from all the active EVs on the road in Shanghai. The trip information based on GPS tracking includes driving location and distance, while the charging information includes the state of charge (SOC, i.e., the remaining battery capacity), charging duration, and price. Table A1 provide summary statistics.

The average driving range of the EV sample has increased over time from 293 km in January 2021 to 332 km in January 2024, reflecting the fact that newer EV models tend to have longer driving range. On a weekly basis, the number of trips per EV increased by 8% from 20.9 in January 2021 to 23.4 in January 2024, while the corresponding weekly driving distance rose by 27%, from 376 km to 477 km.

Second, these increases coincide with improvements in both vehicle range capacity and charging network: the average driving range rose from 293 km to 332 km in winter (+13%), and from 356 km to 378 km in summer (+6%). The improvement of the fast-charging network is shown in Figure 1, which explains why reliance on slow charging declined substantially: the share of drivers who always slow charge fell from 76.9% to 53.6% in winter (-30%), likely reflecting improved availability and reliability of fast-charging infrastructure. This is further supported by a 114% increase in weekly fast-charging frequency per driver in winter

[5]Battery electric vehicles (BEVs) accounted for 71% of the EV stock, and 89% of all new EVs sold in Shanghai in 2024.

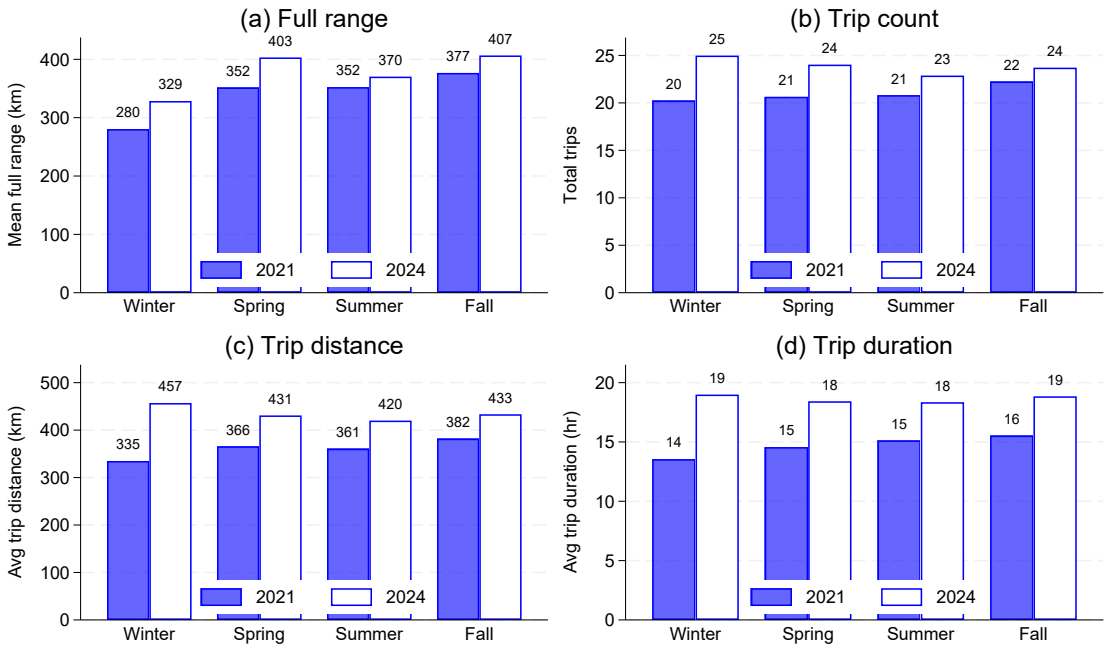
(from 0.7 to 1.5), and by the rise in fast-charging starting SOC from 35% to 40%, suggesting that drivers are using fast charging more proactively rather than waiting until the battery is nearly depleted. In addition to changes from 2021 to 2024, seasonal patterns persist, with winter months consistently associated with longer trip durations, higher trip frequency, and more frequent charging— patterns consistent with higher energy consumption in colder conditions. Overall, the data reflect a clear shift toward more frequent and longer-range EV usage, supported by better-performing vehicles and a growing fast-charging infrastructure. These changes underscore a broader maturation in the EV ecosystem between 2021 and 2024.

Pattern 1: Charging depends on remaining battery Figure 4 provides clear visual evidence that charging behavior is strongly influenced by the remaining battery level. The number of charging events most likely to occur when the stat of charge (remaining battery level) is between 30% and 50%, and sharply declines as the battery level increases. In contrast, driving events (pink bars) are the opposite, and we see more than 80% of trips occur at the battery level $> 50\%$. The green line, representing the fraction of charging events out of all events, falls steadily with battery level, indicating that drivers are significantly more likely to charge when their battery is low, but also exhibit clear dynamic considerations and prefer to maintain battery at relatively high level.

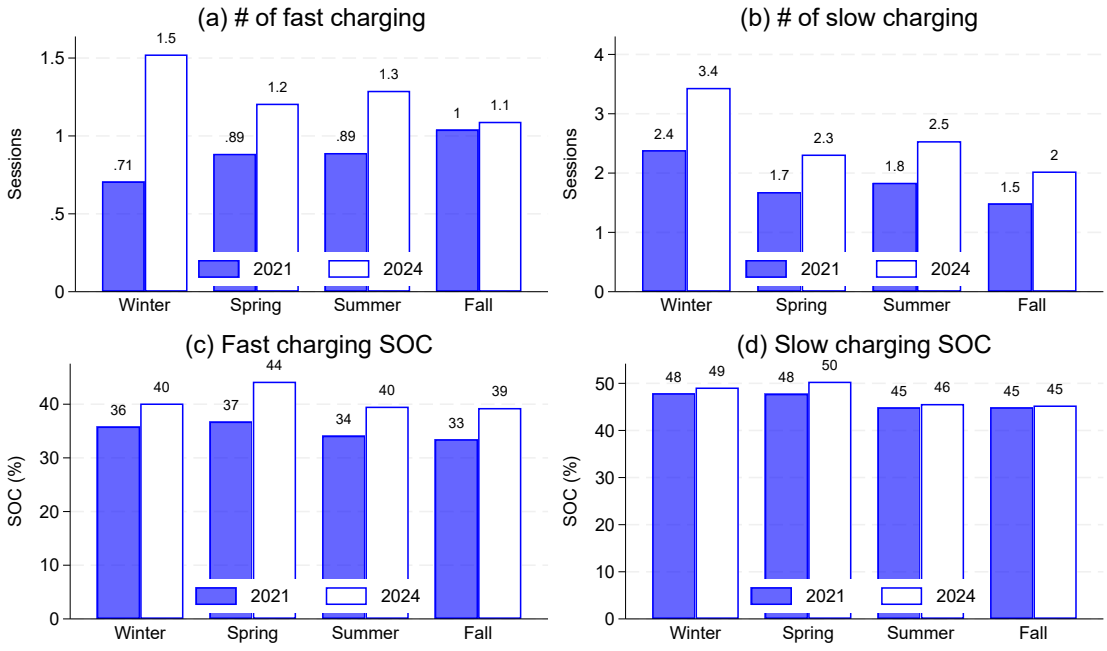
Pattern 2: Charging depends on relative convenience to the charging facility To further analyze how charging decisions depend on other state variables, we define the probability of charging trips as the ratio of charging trips and all trips, and group them in different state bins. To visualize the relationship between charging behavior and local station attributes, I construct binned scatterplots by grouping trip-level observations based on the value of the explanatory variable— either the number of stations within 1 km (Figure 5(a)) or the price at the nearest station (Figure 5(b)). For each bin, I calculate the average probability that a trip is a charging event, separately for low and high battery conditions (defined by whether the state-of-charge (SOC) at trip start is below or above 40%). I then plot these bin averages and overlay a smoothed (quadratic) trend line to highlight the patterns.

Figure 5(a) show the suggests that drivers' charging decisions are influenced by network size, and these effects are stronger when the battery level is low (SOC$<$40%). The probability of initiating a charging trip increases sharply with the number of nearby stations, especially when SOC is below 40%. This indicates that network size enhances charging convenience, and drivers with low remaining battery are particularly responsive to that. They are more likely to initiate charging if several options are within close range, likely due to lower costs (such

Figure 1: Data Description of EV usage dataset: 2021 vs. 2024



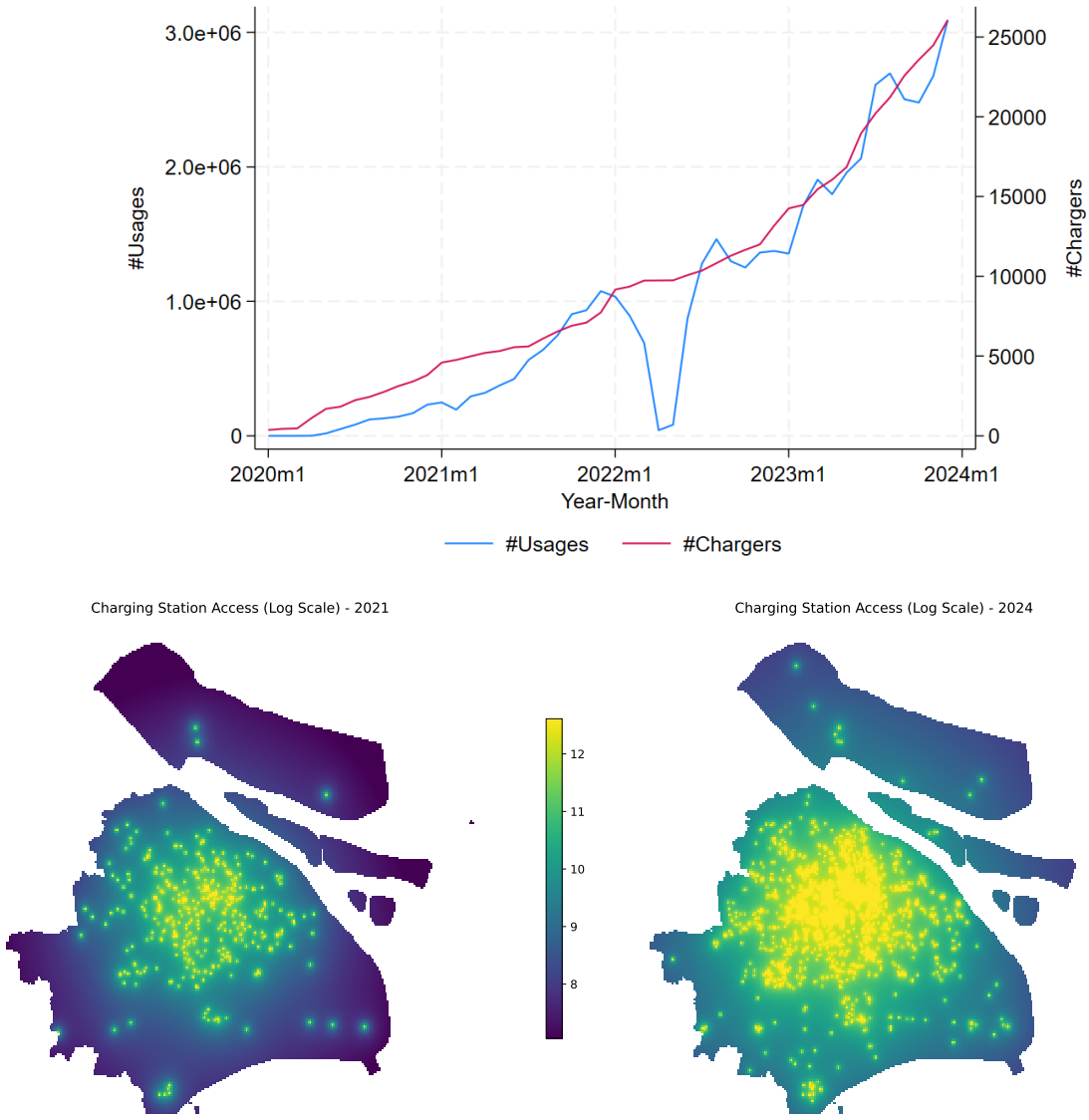
(a) Trip-related events



(b) Charging-related events

Note: The dataset in each year includes four weekly cross-sections of 1100 randomly selected representative EVs in Shanghai during a week in Jan (Winter), March (Spring), Aug (Summer), and Oct (Fall), respectively, for the years 2021 and 2024.

Figure 2: **Fast-Charging Station**: Numbers and Usages

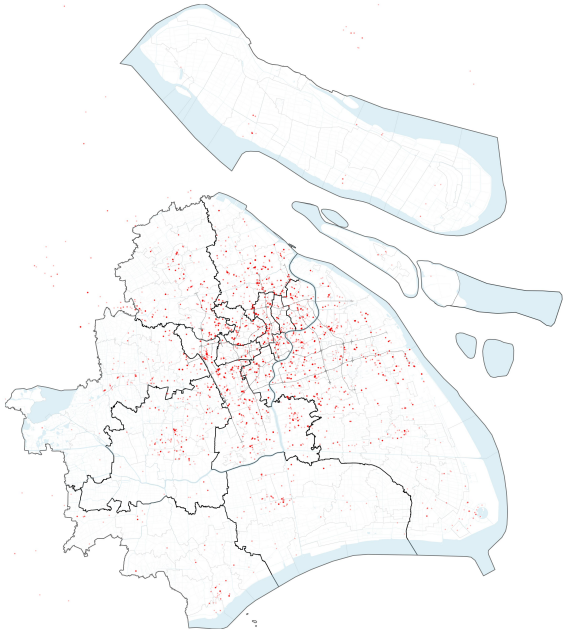


(a) Charging Access (2021)

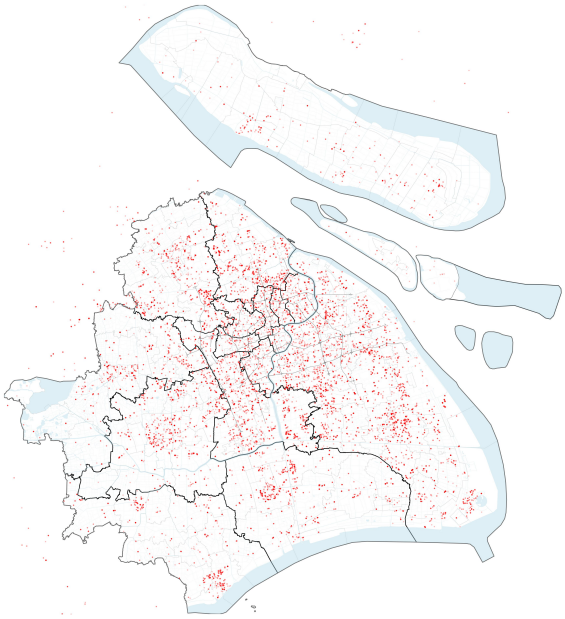
(b) Charging Access (2024)

Note: The top figure shows the number of fast-charging chargers and their number of usages in Shanghai. Bottom Figure (a) and (b) report the log(charging access) of each location measured in 2021 and 2024. Charging access for location i is defined as the sum of the inverse squared distance to fast charging stations i. ($CA_i = \sum_j \frac{1}{dist_{ij}^2}$).

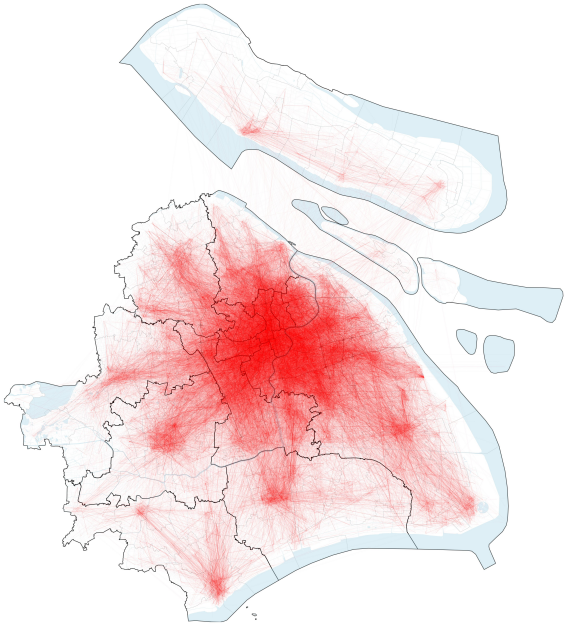
Figure 3: Descriptions of the EV Trip dataset



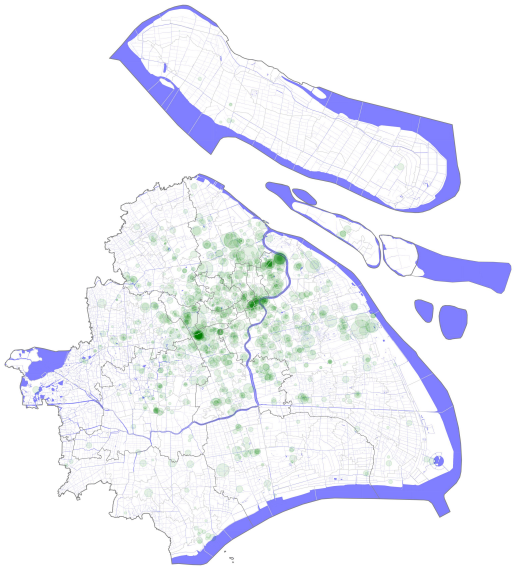
(a) Fast Charging Locations



(b) Slow Charging Location



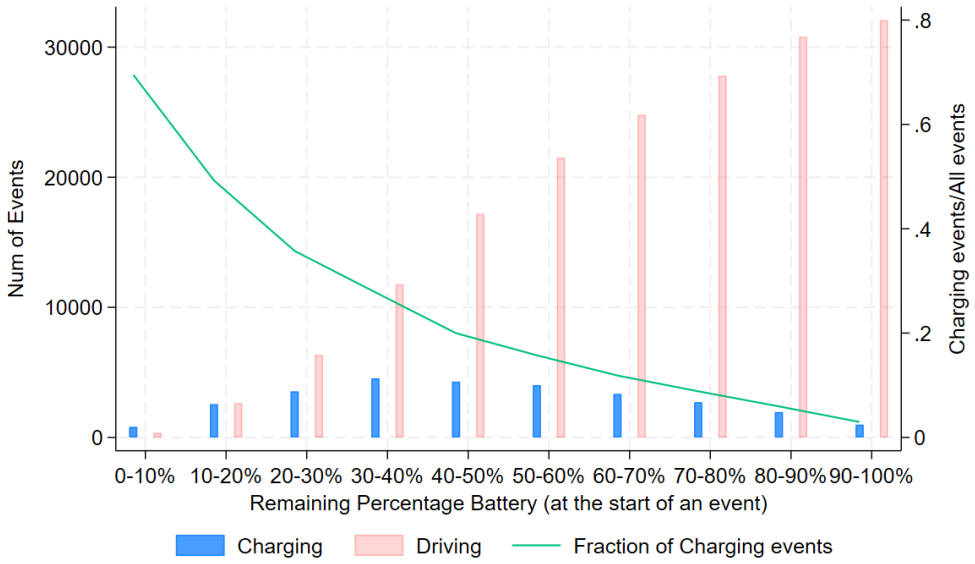
(c) Trip: Origin to Destination



(d) Station (weighted by usage)

Note: Figure (a)-(c) shows the data in the EV trip dataset. Figure (a) plots locations of the observed 8,524 fast charging; Figure (b) plots the locations of the 16,986 observed slow charging; Figure (c) plots the connected lines of 188,707 trip origins to destinations (excluding trips outside Shanghai for visualization). Figure (d) plots the fast charging station usages from the station dataset in 2024 and aligns well with Figure (a), verifying the representativeness of the trip sample.

Figure 4: **Raw data**: #Events in the dataset given each state

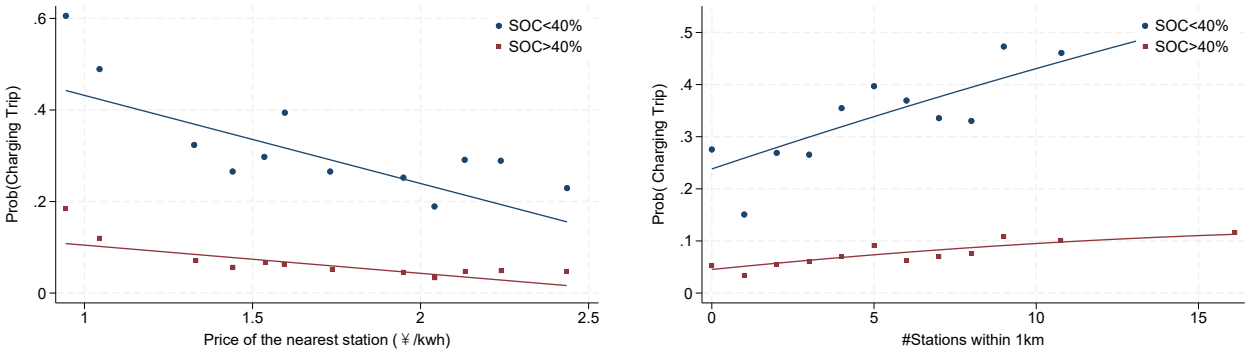


as time costs, hassle costs, and searching costs). In contrast, the relationship is much flatter for drivers with SOC $> 40\%$, who are not as constrained and can afford to delay charging or travel farther.

Pattern 3: Charging depends on prices Figure 5(b) shows that charging probability decreases with price, particularly when SOC is low. This suggests that drivers exhibit price sensitivity, but only when they have some flexibility. For drivers with SOC$<40\%$, there's a clear negative relationship—lower prices increase the likelihood of charging. The same relationship holds when SOC is above 40%, but the slope is smallers (actualy the probability approaches 0 when price is high and the state of charge is high. Together, Figure 5(a) and (b) show that both convenience and monetary incentives shape charging decisions, but these frictions bind more strongly under lower battery conditions.

Pattern 4: Usage reflects range anxiety To characterize the observed usage (trip) patterns, I estimate the rate at which trips transition from one remaining range bin to another. Assuming that trips are taken via a Poisson process with different Poisson rate for a trip from range i to range j (by definition $j \leq i$), I construct Table 6 where each entry (i, j) represents the estimated Poisson rate of trips taken that begin in SOC bin i and end in SOC bin j. Each SOC bin corresponds to a 50km interval of remaining driving range. There are a few takeaways:

Figure 5: Charging behavior as a function of charging network size and price



(a) Charging probability vs. local charging access

(b) Charging probability vs. price at nearest station

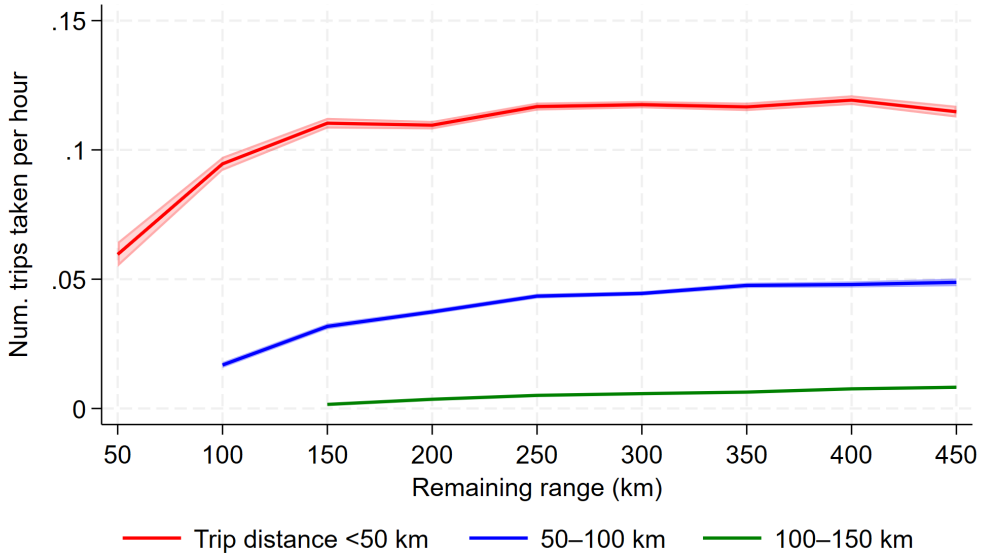
Note: For each trip, I calculate the probability that the trip involves charging and examine how it changes with local station access and price. Two patterns emerge: (1) Consumers are more likely to charge in areas with a dense network. (2) Consumers are more likely to charge at locations with lower prices. In both cases, the effect is stronger when the remaining battery is below 40%.

First, the matrix shows a decreasing arrival rate of trips with distance k (e.g., all entries $(i, i-k)$ for any k): short trips are more common, and long-range transitions occur less frequently. Second, the structure of the matrix shows that trips with distance k (e.g., all entries $(i, i-k)$ for any k) occur with comparable frequency, suggesting that the trip arrival (the need to drive) is likely to be orthogonal to the car conditions. Lastly, we see the arrival rate is comparatively lower for trips ending in very low SOC levels ($<$ 100 km). Lastly, the estimated ex-post trip arrival process shows two downsides of maintaining a low SOC: (1) some trips are not technically feasible, for example, the trip of distance 200km cannot be taken at a starting range of 150km, (2) some feasible trips are chosen to be forgone due to potential range anxiety, for example, a driver with range 200km is reluctant to take a trip of distance 150km because it is risky to do so (e.g. the battery may deplete with some uncertainty).

Table 1: Empirical Test of Range Anxiety: Dependent variable: log(trip hazard rate)

	(1) Baseline	(2) Morning	(3) Weekend	(4) Winter	(5) Summer
1(Remain. range after a trip <50km)	-0.672***	-0.674***	-0.552***	-0.725***	-0.580***
	(0.198)	(0.197)	(0.115)	(0.171)	(0.196)
1(Remain. range after a trip 50-100km)	-0.162	-0.163	-0.113	-0.179***	-0.0813
	(0.108)	(0.108)	(0.137)	(0.0558)	(0.104)
Trip Distance FE	Yes	Yes	Yes	Yes	Yes
R-squared	0.990	0.990	0.993	0.988	0.987

Figure 6: Range Anxiety: hazard rates of trip initiation by remaining driving range

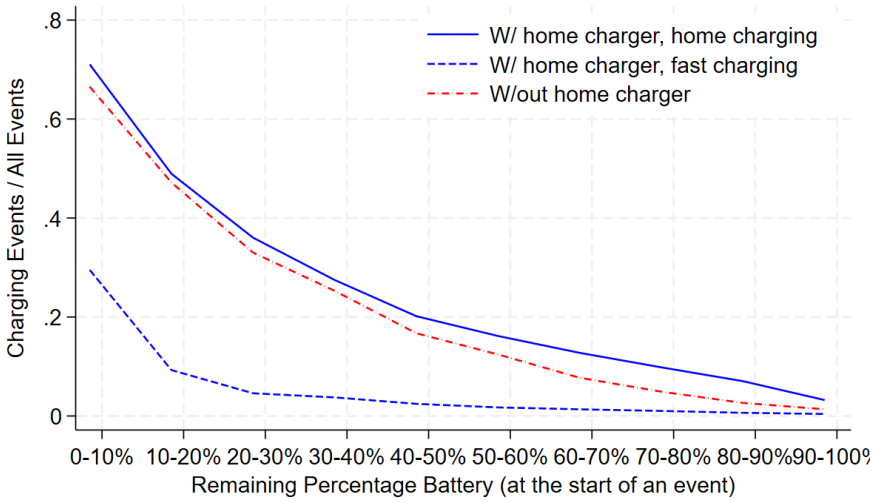


Note: Each colored line corresponds to a trip with a certain distance: < 50 km, 50–100 km, 100–150 km, and 150–200 km. Hazard rates are computed as the number of trips initiated per hour from each starting remaining range (x-axis), normalized by the hours vehicles stay in that state (until a trip arrives). Shaded areas show 95% confidence intervals.

Pattern 5: Difference in charging patterns of drivers with home charger Consumer exhibit different charging patterns. Home chargers primiarily use home chargers, and occasionally rely on fast chargers for urgent needs (for example, long-distance trips). They are less sensitive to remaining battery, show a less steep gradient of charging probability with respect to remaining battery level. They are more likely to charge at high level of remaining battery compared to people without home chargers. This is perhaps due to the convenience of charging at home, so consumers have a relative low cost of keeping battery level high.

When home charging, consumers are also sensitive to prices due to the peak-load pricing scheme. When charging at fast chargers, consumers are less sensitive to the price or compared to people with home chargers, perhaps because they are less familiar with the public charging facilities, also likely because house owners are of higher income.

Figure 7: Charging behavior by remaining battery: with or without home chargers



Notes: This figure plots the distribution of charging events by the remaining percentage of battery at the start of an event. The solid blue line shows home charging for users with home chargers, while the dashed blue line indicates their fast charging behavior. The dashed red line represents users without home chargers. Charging at very low battery levels is disproportionately concentrated among those without home chargers, while users with home chargers tend to charge more frequently at higher remaining battery levels.

3 Empirical Model

3.1 Setup

In light of the data patterns, we write a dynamic model of EV usage in continuous time. There are two advantages of a continuous time model: (1) trips and charging events are intrinsically continuous, continuous time allows us to use the time interval information in the estimation and reduce the discretization bias; (2) we do not need to specify the order of events, and events won't occur simultaneously in the model.

In the model, a representative consumer of type i driving a car with a full range at $\bar{R}_i$, having trips arrive via a Poisson process that is state-dependent. The driver can decide whether to take the trip or not, conditional on the trip's arrival. Taking the trip will shift the state, but also earn the trip utility. The driver also has charging opportunities arrive via a Poisson process, and the driver can decide to charge or not, given the current state. The key model elements are summarized below:

Consumer Types We define various consumer types and assume representative consumers within each type. Each consumer type i is determined based on the full battery range of the car ($\bar{R}$), the charging network size (N, either in 2021 or 2024), and whether the consumer has

access to home chargers (H).

State Variable There are four state variables: $\mathbb{S} = \mathbb{B} \times \mathbb{R} \times \mathbb{P} \times \mathbb{H}$ ($10 \times 4 \times 4 \times 2 = 320.$). Specifically, 1) battery (range in km): $b = \{1, ..., 10.\}$ denoting the remaining battery range level 0-50, 50-100, ..., 450-500km; 2) location convenience: $r = \{1, 2, 3, 4\}$ if the log(charging access) measure in different bins ($CA_i = \sum_j \frac{1}{dist_{ij}^2}$); 3) price: $p = \{1, 1.3, 1.5, 2\}$, corresponding to the frequently observed charging prices in our data; and 4) home: $h = \{0, 1\}$, which takes the value of 1 if the location is near a home charger. This variable is only relevant to consumers with home chargers.

Trip arrival and decisions A trip in our model is characterized as a state transition from s to s'. We need to specify both the frequency of a trip and, conditional on arrival, how state transits. We assume that the arrival of trips is exogenous and shifts the state s to s' at rate $q_{ss'}$. We make the parametric assumptions on how the trip arrival shifts different state variables:

- battery range: The matrix Λ_r represents the state transition probabilities of the battery range induced by trip arrivals. Each entry $(b, b-j)$ in the matrix corresponds to a trip of length j that depletes the battery from level b to level $b-j$.

  We assume that trips of length j (for $j = 0, 1, \ldots, 9$) arrive at a fixed rate λ_j that is *independent of the current battery level* b. In other words, a trip of 0–50 km arrives with the same rate regardless of whether the vehicle's current range is 300 km or 500 km. This assumption is supported by Figure 6.

  As a result, the transition matrix Λ_r exhibits a special (Toeplitz) structure: it is a lower-triangular matrix with constant values along each sub-diagonal. Specifically,

  $$\Lambda_r(b, b-j) = \lambda_j, \quad \text{for all } b \geq j+1, \text{ and } j = 0, \ldots, 9.$$

  All entries above the main diagonal are zero, since the battery cannot increase without charging.

- the probability of a trip from location with charging access (d) to the new location with a charging access (d') is given by $\lambda_{dd'}$. Since there are four states, Λ_d is a 4×4 matrix.

- similarly, the probability of a trip from a location with charging price (p) to the new location with charging price (p') is given by $\lambda_{pp'}$. Since there are four states, Λ_p is a 4×4

matrix.

- Probability of a trip arriving at home chargers is given by $\Lambda_h \in \mathbb{R}^2$.
- We assume the transition process of the four states is independent. The final transition matrix $q_{ss'}$ (state s to state s') is given by:

$$\mathbf{q} \equiv \begin{bmatrix} \lambda_0 & 0 & 0 & \cdots & 0 \\ \lambda_1 & \lambda_0 & 0 & \cdots & 0 \\ \lambda_2 & \lambda_1 & \lambda_0 & \cdots & 0 \\ \vdots & \vdots & \vdots & \ddots & 0 \\ \lambda_9 & \lambda_8 & \lambda_7 & \cdots & \lambda_0 \end{bmatrix} \bigotimes \Lambda_d \bigotimes \Lambda_p \bigotimes \Lambda_h = q_{ss'}$$

- After a trip arrives, the driver decides whether to take the trip or not, and we assume the driver always takes the trip if the remaining battery level is above 300 km (cutoff $\chi = 6$). When below 300 km, the driver will decide based on the utility of the trip from s to k. The utility of taking the trip is given by:

$$\psi(1, s, s') = \alpha_0 + \alpha_1(b_r - b_{r'}) + \alpha_2 \mathbf{1}(r_{s'} = 2) + \alpha_3 \mathbf{1}(r_{s'} = 1) + \varepsilon,$$

  and we normalize $\psi(0, s, s') = 0$ for not taking the trip. α_0 represents the baseline value of a trip, α_1 is the premium for long-distance trips, and α_2 and α_3 capture the anxiety of taking a trip leading to a very low remaining battery range.

- Therefore, the policy of taking the trip is given by:

$$p_{\text{trip}} = \begin{cases} 1, & \text{if } x_r > \chi \\ \frac{\exp[(\psi(1,s,s')+V(s')]}{\exp[\psi(1,s,s')+V(s')]+\exp[\psi(0,s,s')+V(s)]}, & \text{if } x_r \leq \chi, \end{cases}$$

  and the modified (observed) arrival rate is $\tilde{\mathbf{q}} = \mathbf{p} \times \mathbf{q}$.

Charging arrival and decisions The agent decides whether to charge or not, and the opportunity of charging arrives at the opportunity rate λ_c. If charging, pays the costs $c(1, s)$ and move the state back to the battery level s' with probability $p_{s'}$. Otherwise, the new state will be the same as the old state $s' = s$. We parameterize the cost of charging as follows:

$$c(1, s) = \beta_0 + d_s \, \beta_1 + p_s \, \beta_2 + h_s \, \beta_3 + \varepsilon, \qquad c(0, s) = 0.$$

We further assume full recharge when charging, and charging will not move any states other than remaining range r: $s = (r, d, p, h) \rightarrow s' = \bar{s} \equiv (r' = \bar{r}, d, p, h)$. And we define the new state after charging at s as $\bar{s}$.

Therefore, the charging choice probability conditional on an opportunity is given by:

$$\pi_{\text{chg}}(s) = \frac{\exp\big(c(1,s) + V(\bar{s})\big)}{\exp\big(c(1,s) + V(\bar{s})\big) + \exp\big(V(s)\big)}.$$

Other model elements We assume that the flow utility $u(s) = 0$. (Utility only comes from trips.) We set the (continuous time) discount rate at $\rho = 0.1/365 = \frac{1}{\delta} - 1$ per day, which corresponds to the (discrete time) discount rate at $\delta = 0.999726$ per day (or 0.9 per year).

3.2 Bellman equation

The Bellman equation characterizes the value function $V(s)$ in a continuous-time decision process where transitions occur stochastically. The intuition is as follows, consider what can happen in a short time window Δt: the agent accrues an immediate utility flow $u(s)\Delta t$. With probability $q_{ss'}\Delta t$, an exogenous transition (trip) to state s' occurs, yielding a continuation value in the new state s': $V(s')$ and trip value: $\psi(s, s')$. Additionally, with arrival rate λ_c, the agent has a chance to charge the vehicle or choose $j \in \{0, 1\}$ to maximize $c(j = 1, s) + \varepsilon_j + p_{s\bar{s}}(j)V(\bar{s})$ and $c(j = 0, s) + V(s)$, incorporating random shocks ε_j. The probability of nothing arriving and remaining in state s is $1 - \sum_{s' \neq s} q_{ss'}\Delta t - \lambda_c \Delta t$. We discount all future rewards at rate ρ. And the resulting Bellman equation is:

$$\begin{aligned} V(s) = u(s) \times \Delta t + \sum_{s'} \frac{q_{ss'}\Delta t}{1 + \rho \Delta t} E \max_{j \in \{0,1\}} \Bigg\{ & \underbrace{\psi(j = 1, s, s') + V(s') + \epsilon_1}_{\text{travel}}, \underbrace{\psi(j = 0, s, s') + V(s) + \epsilon_0}_{\text{not travel}} \Bigg\} \\ & + \frac{\lambda_c \Delta t}{1 + \rho \Delta t} E \max_{j \in \{0,1\}} \Bigg\{ \underbrace{c(j = 1, s) + \varepsilon_1 + V(\bar{s})}_{\text{charging}}, \underbrace{\varepsilon_0 + V(s)}_{\text{not charging}} \Bigg\} \\ & + \frac{1 - \sum_{s'} q_{ss'}\Delta t - \lambda_c \Delta t}{1 + \rho \Delta t} V(s). \end{aligned}$$

This equation approximates a continuous-time Hamilton-Jacobi-Bellman (HJB) equation as $\Delta t \to 0$. Solving the equation yields:

$$
\begin{aligned}
V(s) =& \frac{u(s) + \sum_{s'} q_{ss'} \log \left[\exp(\psi(1, s, s') + V(s')), \exp(V(s')) \right]}{\lambda_c + \rho + \sum_{s'} q_{ss'}} \\
&+ \frac{\lambda_c \log \left[\exp(\frac{c(1,s) + V(\bar{s})}{\sigma}) + \exp(\frac{V(s)}{\sigma}) \right] + \lambda_c \gamma}{\lambda_c + \rho + \sum_{s'} q_{ss'}}
\end{aligned} \tag{1}
$$

3.3 Estimation Details

We follow a two-step estimation procedure. We recover the state arrival and transition in the first stage by estimating a hazard-rate model based on the observed trip arrivals and transitions and the time interval between these events. In the second step, we evaluate the empirical likelihood of observed trip-taking and charging probabilities at different states. The idea is similar to the discrete-type dynamic model, but the main advantage is that we will make use of the time interval between events in a continuous measure (which sheds light on the hazard rates) and do not need to specify the order of each event.

Step 1: Estimating the Reduced-Form Arrival rates (Transition probabilities) Let q_{kl} denote the hazard rate of a natural transition from state k to l. Our setting includes the state transition hazard rates and given different states (battery levels, locations, and prices).

In state k, the probability of the next stage change occurring within τ units of time is,

$$
1 - \exp\left[-\tau \left(\sum_{l \neq k} q_{kl} \right) \right], \tag{2}
$$

and the probability of the next stage change not occurring within τ units of time is,

$$
\exp\left[-\tau \left(\sum_{l \neq k} q_{kl} \right) \right] \tag{3}
$$

This is the cumulative distribution function (cdf) of the exponential distribution with a rate parameter equal to the sum of the exogenous state transition rates and the hazards of the player. Differentiating with respect to τ yields the density for the time of the next state change, which is the exponential probability density function with the same rate parameter as before:

$$\left(\sum_{l\neq k} q_{kl}\right) \exp\left[-\tau\left(\sum_{l\neq k} q_{kl}\right)\right]. \tag{4}$$

Now, define g to be the exponential term restated as a function of h :

$$g(\tau, k; \lambda) = \exp\left[-\tau\left(\sum_{l\neq k} q_{kl}\right)\right].$$

And the corresponding likelihood of nature moving the state from k to l being:

$$q_{kl} g(\tau, k; \lambda)$$

Now consider a continuous time sample of M agents making N state transitions in the sample. Define $I_{mn}(0, l)$ as the indicator for whether the n-th move of driver m to state l due to the trip arrival, and $I_{mn}(1, l)$ if the arrival to state l is due to charging or period n is the last observation in the sample period. Define $\tau_{mn} \equiv \underline{t}_{mn} - \bar{t}_{m,n-1}$ to be the holding time between two events. For the interval between the last event and the end of the sampling period, we define the final state and interval length as $k_{m,T+1} \equiv k_{m,T}$ and $\tau_{m,T+1} \equiv \bar{T} - t_{mT}$. Then, the maximum likelihood estimates of the hazards $\mathbf{q}$ are

$$\hat{\mathbf{q}} = \arg\max_{h\in\mathcal{H}} \left\{ \sum_{m=1}^{M} \sum_{n=1}^{T} \left[\sum_{l} (I_{mn}(0, l)) \left(\ln g\left(\tau_{mn}, k_{mn}; \mathbf{h}\right) + \ln q_{kl}\right) \right] + \sum_{l} (I_{mn}(1, l)) \ln g\left(\tau_{mn}, k_{mn}; \mathbf{h}\right) \right\}$$

The last term is the natural log of one minus the exponential cdf, to account for the fact that another state change was not observed before a charging event. Because consumers may exhibit range anxiety and forgo trips that lead to low battery level, the observed trip transitions to low battery level may be underestimated. Therefore, we just focus on the trips with initial remaining range $>$ 300km for the estimation on the transition probabilities.

Step 2: Estimating the Structural Parameters Given structural parameters $\theta = \{\boldsymbol{\alpha}, \boldsymbol{\beta}\}$ and hazard rates estimated in the first stage, we can solve the state-dependent value function via value function iteration as defined in (1): $T : V(k) \to V(k)$.

Then we can then express the policy $\hat{h}_{ijk}$ ($j = 1$, or charging) and $\hat{p}_{ijks}$ ($j = 1$, or travelling)

as a function of estimated hazard rate $\hat{\mathbf{q}}$ and structural parameters $\theta = \{\boldsymbol{\alpha}, \boldsymbol{\beta}\}$.

$$\hat{\pi}_{i1k}(\hat{\mathbf{q}}, \theta) = \frac{\exp[c(1,s) + \sum_k p_{sk} V(k)]}{\exp[c(1,s) + \sum_k p_{sk} V(k)] + \exp(c(0,s) + V(k))}$$

The joint likelihood of the next state change occurring after an interval of length τ and being the result of driver i taking charging action j is

$$\hat{\pi}_{ijk}(\hat{\mathbf{q}}, \theta) \hat{g}(\tau, k; \hat{\mathbf{q}}, \theta)$$

In addition, drivers decide on taking the trip or not, we need to estimate the policy function of taking trips $\hat{p}_{ijks}$ ($j = 1$, or taking the trip from k to s) as:

$$\hat{p}_{i1ks}(\hat{\mathbf{q}}, \theta) = \frac{\exp[\psi(1,k,s) + V(s)]}{\exp[\psi(1,k,s) + V(s)] + \exp(V(k))} \text{ if } b_s \leq \chi$$
$$\hat{p}_{i1ks}(\hat{\mathbf{q}}, \theta) = 1 \text{ if } b_s > \chi$$

The joint likelihood of the next state change occurring after an interval of length τ and being the result of driver i taking traveling action $j = 1$ to state s is

$$\underbrace{\hat{q}_{ks} \hat{p}_{i1ks}(\tilde{\mathbf{q}}, \theta)}_{\tilde{q}_{iks}} \hat{g}(\tau, k; \tilde{\mathbf{q}}, \theta)$$

For driver m and all the observed actions n (trip/charging), we define $I_{mn}(c, j) = 1$ if the state change at period n is a result of charging decision, $I_{mn}(t, j) = 1$ if the state change at period n is a result of traveling decision to state s. The second stage MLE estimates can be written as:[6]

$$\hat{\theta} = \arg\max_{\theta} \left\{ \sum_{m=1}^{M} \sum_{n=1}^{T} \left[\ln \hat{g}\left(\tau_{mn}, k_{mn}; \hat{\mathbf{q}}, \theta\right) + \sum_i \sum_{j \neq 0} [I_{mn}(c,j)] \ln \hat{\pi}_{ijk}(\hat{\mathbf{q}}, \theta) \right.\right.$$
$$\left.\left. + \sum_i \sum_{j \neq 0} [I_{mn}(t,j)] \ln \tilde{q}_{iks}(\hat{\mathbf{q}}, \theta) \right] + \ln \hat{g}\left(\tau_{m,N+1}, k_{m,N+1}; \tilde{h}, \theta\right) \right\}$$

[6] For the interval between the last event and the end of the sampling period, we define the final state and interval length as $k_{m,T+1} \equiv k_{m,T}$ and $\tau_{m,T+1} \equiv \bar{T} - t_{mT}$.

4 Estimation Results

The goal is to recover hazard rate parameters: $\mathbf{q} = \{q_{jk}\}$ (state transition probabilities), and structural parameters $\{\boldsymbol{\alpha}, \boldsymbol{\beta}\}$. The results are shown in Table 2, Table 3, and Figure 8.

4.1 Model Estimates

Trip Arrival Estimates. The left panel of Table 2 reports the estimated Poisson arrival rates of trips per day, segmented by driving distance. The estimates reveal that short trips are much more frequent than long ones: trips under 50 km occur at a rate of 2.64 per day, while 50–100 km trips occur at 1.41 per day. In contrast, trips exceeding 200 km are rare, with arrival rates quickly dropping below 0.05 per day. This pattern aligns with observed EV usage behavior, where drivers most commonly make short-distance trips for commuting and errands, and only occasionally undertake long-range travel due to range limitations, planning requirements, and charging constraints.

Trip Transition Frequencies. The left-bottom panel documents empirical frequencies of arriving at different types of destinations, defined by charging access measure (CA) and charging price, in 2021 and 2024. In 2021, a higher share of trips went to low-access, high-price areas— possibly reflecting uneven network development. By 2024, the trip usually led to locations with good charging access, indicating improved spatial distribution of the charging network.

Trip Utility Parameters. Panel A of Table 3 presents structural parameters governing the utility of taking a trip as a function of trip distance. The base utility of short trips ($\alpha_0 = 2.8549$) is high, reflecting the fact that trips are routine and often necessary and forgoing trips are costly. Longer trips are more valuable ($\alpha_1 = 0.7992 > 0$. Trips leading to low battery level generate disutility. In particular,($\alpha_2 = -0.7512$ for (50–100 km) , $\alpha_3 = -1.9424$ for 0–50 km). These estimates help rationalize the steep drop in observed realized trip frequencies for trips that lead to low battery levels.

Charging Cost Estimates. Panel B of Table 3 summarizes estimates for the cost of charging for drivers without home chargers. The baseline fixed cost of initiating a charge is negative ($\beta_0 = -2.55$), indicating that consumers incur a hassle cost around ¥51 per fast-charging (assuming 30 kWh per charge). However, this disutility is mitigated when a charging station is conveniently located nearby: $\beta_1 = 0.70$ shows that increasing charging access significantly

Table 2: Model Estimates: State Arrival & Transition

	W/out H.C.		W/ H.C.	
	Estimate	SE	Estimate	SE
Trip Arrival (per day)				
<50km	2.8316	(0.7336)	2.7081	(0.6613)
50-100km	1.2479	(0.2429)	1.0021	(0.1207)
100-150km	0.2263	(0.9280)	0.1127	(0.0782)
150-200km	0.0941	(0.3045)	0.0323	(0.1303)
200-250km	0.0382	(0.4521)	0.0101	(0.1833)
250-300km	0.0193	(0.8336)	0.0037	(0.2669)
300-350km	0.0098	(0.4888)	0.0013	(0.8633)
350-400km	0.0039	(0.9682)	0.0007	(0.9514)
400-450km	0.0013	(1.1562)	0.0007	(1.0613)
Probability to a location (2021)				
CA $\in [0, 1]$	0.4181	(0.2431)	0.5037	(0.0670)
CA $\in [1, 2]$	0.3277	(0.1366)	0.3130	(0.0482)
CA $\in [2, 3]$	0.1443	(0.1168)	0.1213	(0.0595)
Price $\in [0, 1.2]$	0.2498	(0.1153)	0.2617	(0.0516)
Price $\in [1.2, 1.5]$	0.1717	(0.0505)	0.2017	(0.0329)
Price $\in [1.5, 2]$	0.2968	(0.0822)	0.2733	(0.0449)
Probability to a location (2024)				
CA $\in [0, 1]$	0.1719	(0.2028)	0.2256	(0.0944)
CA $\in [1, 2]$	0.0984	(0.1170)	0.1741	(0.0638)
CA $\in [2, 3]$	0.2555	(0.1388)	0.2770	(0.0908)
Price $\in [0, 1.2]$	0.2887	(0.2210)	0.2754	(0.0381)
Price $\in [1.2, 1.5]$	0.1849	(0.0791)	0.2272	(0.0448)
Price $\in [1.5, 2]$	0.2700	(0.1433)	0.2471	(0.0678)
Probability to home charger				
Home	0.8015	(0.0338)	0.8015	(0.0338)

Notes: The Number of observations is 8000 drivers with 214,000 sessions. The table reports estimated Poisson trip arrival rates and transition probabilities by types (with or without home chargers, under the 2021 or 2024 network).

reduces the perceived cost. In contrast, high prices impose a substantial penalty, as indicated by $\beta_2 = -1.48$. These estimates are consistent with economic intuition in the data pattern: consumers value convenience and are sensitive to charging prices, especially when they are not urgently in need of energy. Based on the structural estimates, we can compute the elasticity of charging given a uniform increase in the charging price (in all stations) to be -0.98.

Panel C of Table 3 summarizes estimates for the cost of charging for drivers with home chargers. Home drivers can choose to charge with a slow charger (if they are at home) or a fast charger. The hassle cost of charging at home is close to zero ($\beta_3^h \approx 0$), while the hassle

Table 3: Model Estimates: Structural Primitives

Parameter	Estimate	SE
Trip utility		
α_0 (baseline trip utility)	2.4817	0.0129
α_1 (marginal utility per km)	0.8506	0.0155
α_2 (anxiety: 50–100 km remaining)	-0.7881	0.0206
α_3 (anxiety: 0–50 km remaining)	-1.9107	0.0372
Charging cost: consumers without home chargers		
β_0 (base charging disutility)	-2.5470	0.0265
β_1 (sensitivity to charging access)	0.7011	0.0103
β_2 (sensitivity to charging price)	-1.4823	0.0164
Charging cost: consumers with home chargers		
β_0^h (base charging disutility using fast charger)	-4.4599	0.0191
β_1^h (sensitivity to charging access using fast charger)	0.0638	0.0102
β_2^h (sensitivity to charging price using fast charger)	-0.7222	0.0121
β_3^h (base charging disutility using home charger)	-0.0327	0.0215
β_4^h (sensitivity to charging access using home charger)	-0.0173	0.0136
β_5^h (sensitivity to charging price using home charger)	-1.8517	0.0138

Notes: The number of observations is 8,000 drivers with 214,000 sessions. Table 2 reports estimated Poisson trip arrival rates by types (with or without home chargers) across trip characteristics and destination cost intervals. Table 3 reports the estimated structural parameters: Consumers without home chargers: $C(\text{charging}, s) = \beta_0 + \beta_1(\text{CA}) + \beta_2(\text{price})$. Consumers with home chargers: $C(\text{charging}, s) = \mathbb{1}(\text{not home}) \times (\beta_0^h + \beta_1^h(\text{CA}) + \beta_2^h(\text{price})) + \mathbb{1}(\text{home}) \times (\beta_3^h + \beta_4^h(\text{CA}) + \beta_5^h(\text{price}))$. Utility from trips: $\psi(\text{trips}, k, s) = \alpha_0 + \alpha_1(\text{trip distance}) + \alpha_2 \mathbf{1}(b_k \in [50, 100]) + \alpha_3 \mathbf{1}(b_k \in [0, 50])$, where b_k denotes the remaining range level after fulfilling the trip and α_2 and α_3 characterizes range anxiety.

cost of charging at fast chargers is much more expensive ($\beta_0^h = -4.46$, or ¥184 per fast-charging assuming 30 kWh per charge). Consumers are less sensitive to fast charging prices ($\beta_2^h = -0.72$) perhaps because less familiarity with fast-charging networks) but more sensitive to home charging (electricity) prices ($\beta_5^h = -1.85$). Charging access is irrelevant for home charging and matters for fast charging, but much less so ($\beta_1^h = 0.06$). Overall, for consumers with home chargers, the average elasticity of charging probability with respect to charging price is -0.90, and therefore, they are less price sensitive.

Model fit. Model fit is validated in Figure 9 and our model captures the key features in the data: range anxiety reflects the missing trips that lead to low remaining ranges, quickly diminishing charging probability as remaining range is large, sensitivity to price, and local charging access.

4.2 Estimated Policy Functions

Figure 8 illustrates the estimated policy functions governing charging and travel decisions under various battery levels and station attributes. We have different types of consumers, and we start by reporting drivers with an EV full range of 500km, without home chargers (relying on fast chargers), and fixing the station network size at the 2024 level.

Panel (a) shows that the probability of charging declines as the remaining range increases, consistent with rational battery management behavior. However, this decline is highly sensitive to both station access and price: drivers are most likely to charge when stations are dense and prices are low (blue dashed line), and least likely when stations are sparse and prices are high (yellow dashed line). This confirms that both accessibility and affordability play important roles in charging behavior.

Panel (b) extends the analysis by comparing charging probabilities across consumers with different battery types. The curves are closely aligned, suggesting that the general shape of the charging policy is preserved across EVs with different maximum ranges. However, vehicles with greater battery capacity is less likely to charge given the same remaining battery ratio, indicating advantages of larger battery.[7] But they are more likely to charge given the same remaining range because the higher option value of recharging to the full range.

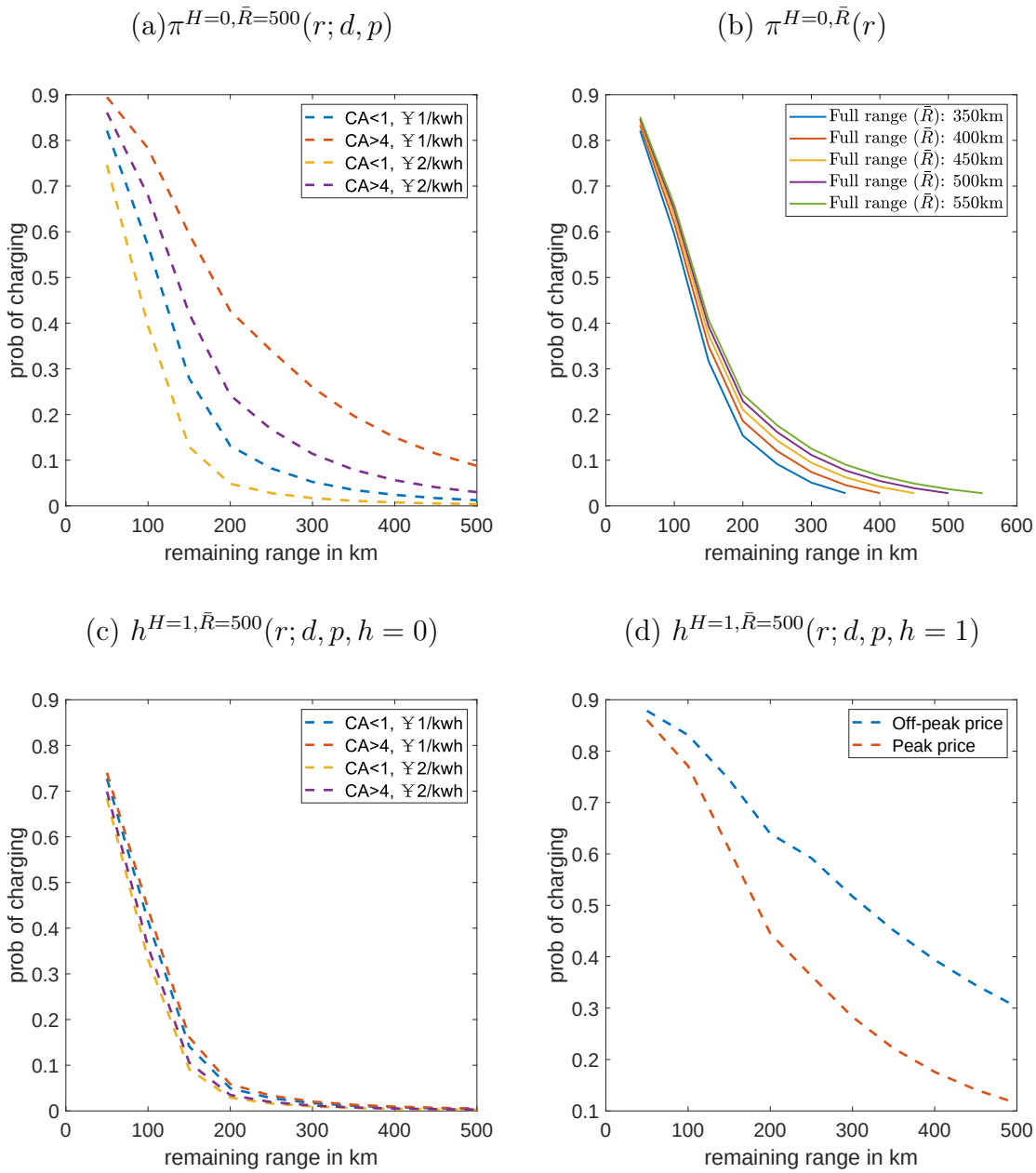
Panel (c) plots the same function as Panel (a), but shows consumers with home chargers deciding whether or not to take a fast-charging opportunity. Consumers are very unlikely to charge when the remaining range is high (> 200 km) because they have the home charging as the back-up option. Consumers are also less sensitive to prices or access, perhaps because they use these stations less frequently, and they would use them only in rare and urgent occasions.

Panel (d) shows consumers with home chargers decide whether or not to take a fast-charging opportunity. The decision rules are quite different— because home chargings are convenient so consumers tend to charge even when the remaining range is very high. Consumers are still sensitive to peak-load pricing and are more likely to charge at off-peak hours.

Appendix Figure A2 presents the estimated travel policy as heat maps. Cells report the conditional probability of taking a trip that transitions the remaining range from the x-axis value to the y-axis value, holding other location attributes fixed. Panel (a) considers trips from the most attractive origins (low prices, high access) to the least attractive destinations; probabilities are near zero at low remaining range, indicating pronounced range anxiety under poor charging conditions. Panel (b) reverses the direction—least attractive to most attractive—

[7] This is to say, a car with full range at 500km is less likely to charge when the remaining range is 250km (50%) compared to a car with full range at 400km to charge at 200 km (50%).

Figure 8: Estimated policy function $h(b, d, p, h)$

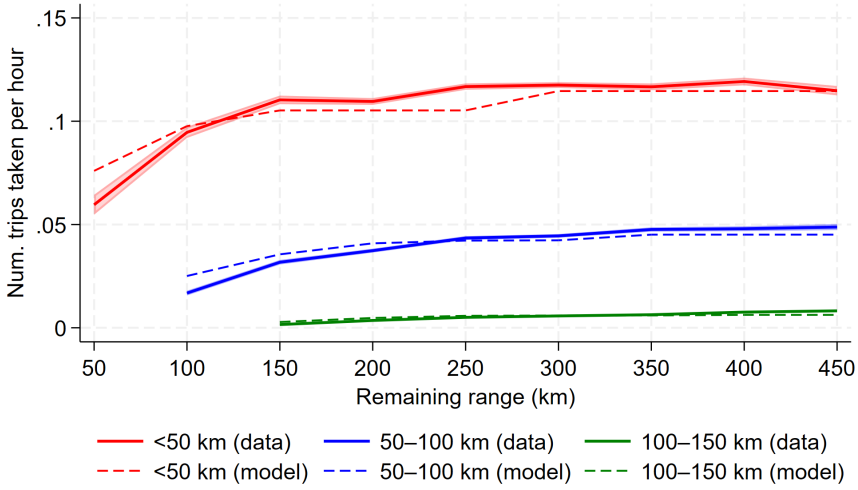


Notes: This figure presents the estimated policy functions $h(b, r, p, h)$ governing charging decisions as a function of b (remaining battery range), d (charging access), p (charging price), and h (home charger nearby). Panel (a) shows the charging probability for consumers without home chargers as a function of remaining range under four scenarios defined by price and station access. Panel (b) shows charging probabilities for consumers without home chargers across the different battery capacities. Panels (c) and (d) display the probability of charging for consumers with home chargers. The probability of using fast-charging is low (close to zero when range $>$ 200km). Charging at home is frequent even when the remaining battery is relatively high and during off-peak hours.

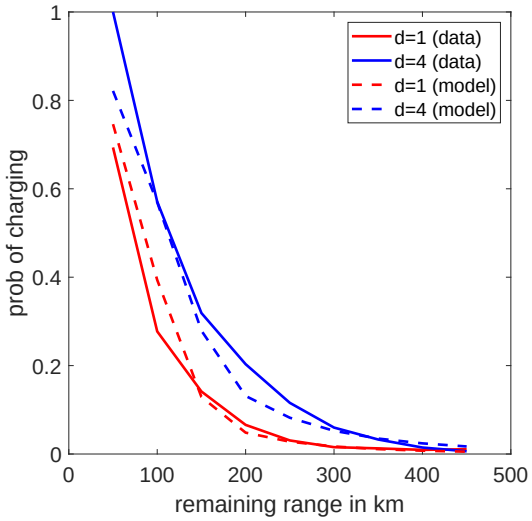
and probabilities are high even at very low remaining range, consistent with more observed trips toward cheaper, better-served areas at low remaining range. Overall, the policy is highly responsive to both remaining range and location variation in charging prices and access.

Figure 9: Model Fit: Estimated Trip-taking hazard rate

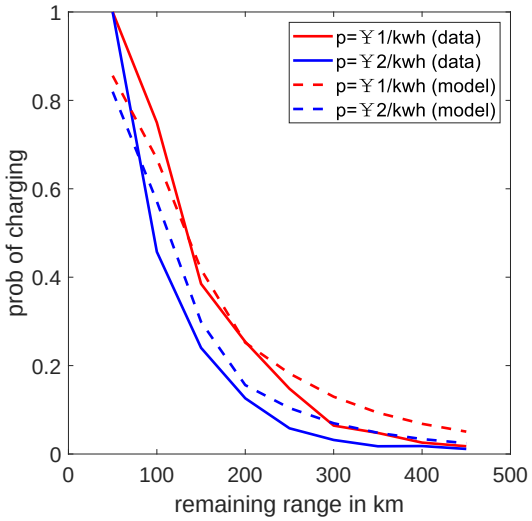
(a) Travelling policy by trip distance



(b) Charging policy by charging access



(c) Charging policy by charging price



Notes: This figure presents the estimated policy functions governing charging and traveling decisions. Solid lines denote policy recovered from data, and dashed line denotes model estimates.

5 Quantification and Policy Simulations

We evaluate counterfactual changes in battery technology and charging infrastructure by monetizing the model's value function—interpreted as the lifetime utility of vehicle ownership. The two policy levers are battery capacity and public charging-station network size. Consumers' willingness to pay (WTP) for them stems from three channels: (i) more realized trips that were previously infeasible or forgone, (ii) lower charging "hassle" (time, detours, queueing), and (iii) improved charge timing that reallocates charging toward cheaper, better-access loca-

tions. We also construct a narrowly defined range-anxiety metric as the dollar value of forgone trips, as a function of the full range of a car and the network size.

To compute WTP, we focus on the ex-ante value function $V(s)$ at the steady state (a vector $\pi(s)$ denoting the probability of being at state s at any point of time) of the continuous-time Markov process:

$$V = \sum_s \pi(s)V(s)$$
$$\text{where } \pi \times Q = \pi,$$

where Q is a transition rate matrix, a function of $\tilde{\mathbf{q}}$ and charging rates $\mathbf{h}$.[8] We numerically simulate $\frac{dV}{dp}$ and this allows us to convert the value function changes to money as the changes in charging prices by computing $\Delta p = \Delta V / \frac{dV}{dp}$ at steady state.

If the model implied that a representative driver will give up Δp in charging price, the annual additional charging cost is: Lifetime WTP $= \Delta p \cdot \frac{D_{\text{year}}}{\bar{E}}$, where $\bar{E}$ is the average range per kWh of electricity and D_{year} is the longtime driving range of an EV. We further assume that $D = 20000 \times 8$, $\bar{E} = 6$. So we can convert the changes in charging prices to changes in lifetime WTP.

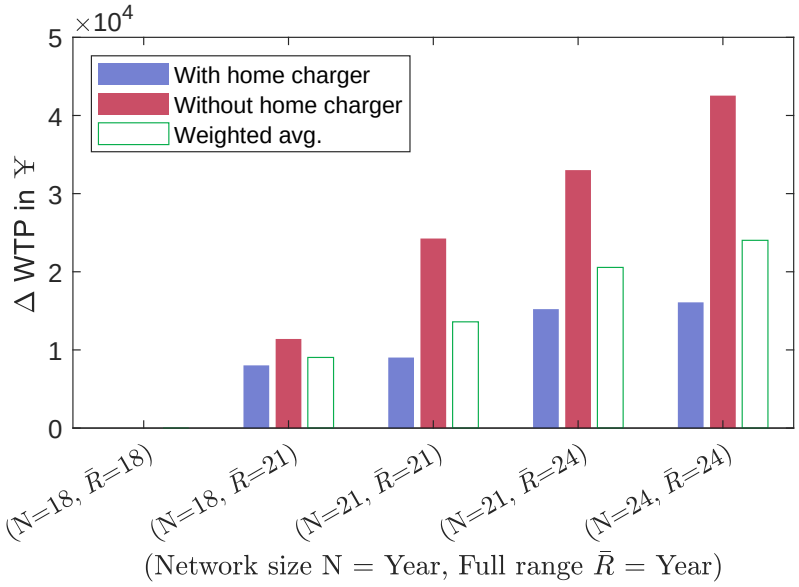
5.1 WTP and Decomposition

We start with a decomposition exercise: how much does the WTP of driving an EV change from 2018 to 2021 to 2024? There are a few big changes: (1) expansion of charging facility (from CA 2.08 to 2.84), (2) longer ranges (average ranges increase from 350km to 400km, (3) cheaper charging prices (average price drops from ¥1.66 to ¥1.62). We show how each policy changes explain the changes in WTP in Figure 10.

Main findings. Figure 10 shows monotonic increases in ΔWTP from 2018 to 2021 and 2024. The largest step occurs when public charging access rises (d: 18→21), while battery upgrades (b: 18→21 and b: 21→24) contribute smaller but positive increments. Gains are much larger for households without home chargers—about 2–4× those with home charging—reflecting their reliance on public infrastructure. Aggregating by observed home-charging shares, the weighted average reaches ≈ ¥30,000 by 2024 (¥62,000 for without home chargers and ¥18,000 for with home chargers).

[8] In a continuous-time Markov process, the transition rate matrix Q describes the rate at which the process moves from one state to another, with each row summing to zero. The off-diagonal elements $q_{ij} \geq 0$ for $i \neq j$, and each diagonal element satisfies $q_{ii} = -\sum_{j \neq i} q_{ij}$, so that each row of Q sums to zero.

Figure 10: Decomposition of welfare gain: 2018 vs. 2021 vs. 2024



Note: Bars show ΔWTP (lifetime WTP, 10,000 ¥) relative to 2018 (N=18, $\bar{R}$=18) as $(N, \bar{R})$ are sequentially updated to 2021 and 2024: at each x-tick, first raise $\bar{R}$ holding N fixed, then raise N holding $\bar{R}$ fixed. Colors: blue = with home charger; red = without; green = sample-weighted mean (weights = observed home-charger shares at 67%).

Simulation Algorithm To conduct counterfactual analysis, we fix the arrival probability of trips of different lengths, and change the state variable to evaluate the new valuation function.

For battery sizes, we shift the battery sizes from 250km to 600km. $B_r = 200km + 50km \times r$, $r \in \{1, 2, ..., 8\}$. This covers the range of most EVs on the market. The full battery capacity would affect the maximum range after a full recharge.

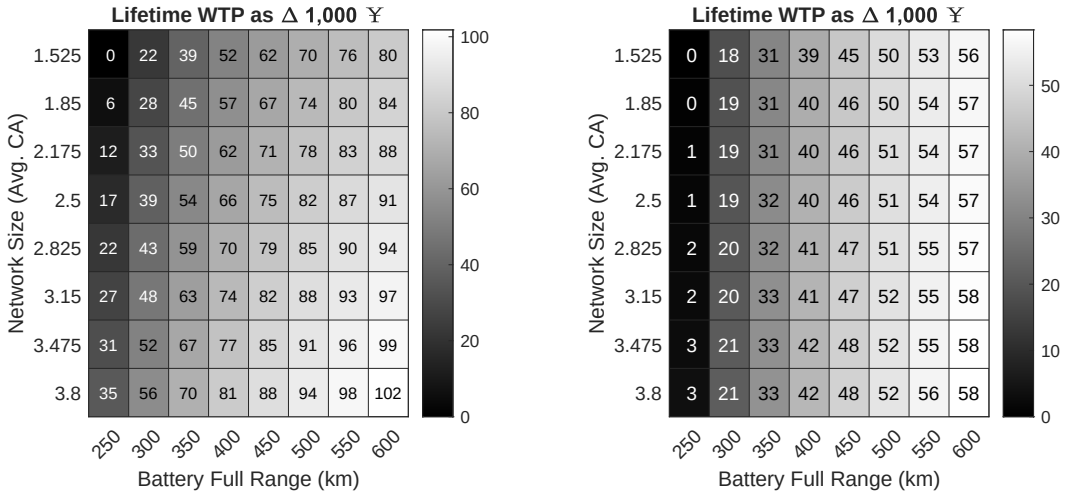
For station access, we shift the probability of distribution of regions (from lowest access to highest access) in the following way: $\theta_r = [0.80.20.00.0] + [-0.1, -0.02, 0.02, 0.1] \times r$ and $r \in \{1, 2, ..., 8\}$. So by shifting r up, we simulate a market with bad access to one with better access. For reference, the current average charging access at the 2021 level is 2.08, and the 2024 level is 2.84.

WTP for Charging Access and Driving Range Panel (a) of Figure 11 reports lifetime WTP (in ¥) for joint increases in battery full range and network size (average charging access, CA). Values are normalized so that the baseline—250 km range and CA = 1.525—has ΔWTP = 0.

First, WTP rises quickly at low levels of range and CA and reaches economically meaningful

Figure 11: WTP for driving range and charging access

(a) Δ WTP without home chargers (b) Δ WTP with home chargers



Notes: Figure (a) shows the estimated willingness to pay (WTP) for network size (or higher average charging access) and the full driving range, both expressed in terms of lifetime charging costs. The baseline in Panel (a) is 100% battery as the current level and the current charging access (CA) level. 2021 network has CA=2.08 and 2024 network has CA=2.84. Panel (b) shows the surplus loss from ("narrowly defined") range anxiety, i.e., people forgo trips that are technically feasible, computed as the difference of the value function when trips are always taken, converted to lifetime WTP.

sizes. For example, at 250 km and CA = 1.85, ΔWTP = 6,000 ¥, while at 600 km and CA = 3.80 it reaches about 102,000 ¥.

Second, holding CA fixed at 1.525, raising the range from 250 to 300 km increases WTP by 22,000 ¥, whereas 550 to 600 km adds only 4,000 ¥. Holding range fixed at 250 km, increasing CA from 1.525→1.85 yields a gain of 6,000 ¥, while 3.475→3.80 adds 4,000 ¥. Thus, both range and network size display diminishing marginal value, though the extra benefits from range diminish faster.

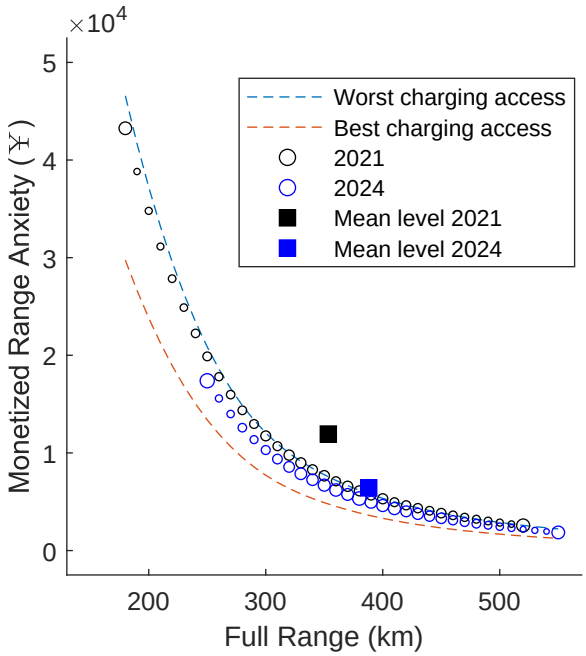
Lastly, range and network size act as substitutes (negative cross-derivatives). From the baseline, increasing only the battery to 500 km yields 70,000 ¥; increasing only CA to 2.825 yields 22,000 ¥. Doing both together yields 85,000 ¥, which is less than the sum of separate effects (92,000 ¥). Intuitively, extra range is most valuable when access to charging is scarce, and improvements in charging access are most valuable when range is limited.

5.2 Quantifying Range Anxiety

In this section, we estimate the magnitude of range anxiety in monetary term, capturing the utility loss from forgone trips that are technically feasible but not taken due to fear of getting stranded on the road. In the model, α_2 and α_3 capture the disutility of taking trips that lead

to a low battery. The utility losses from range anxiety are computed as the difference in the value function between the baseline model and a counterfactual where $\alpha_2 = 0$ and $\alpha_3 = 0$, and therefore all feasible trips are assumed to always be taken.

Figure 12: Range Anxiety by Driving Range



Notes: Each panel plots *monetized range anxiety* (lifetime WTP, 10^4 ¥) against the vehicle's full range (km). Circle area is proportional to the empirical frequency of each full-range level in that year's EV sample. Filled squares mark the weighted mean level for the year. The downward slope indicates that range anxiety declines with battery range; the downward shift from 2021 to 2024 reflects improvements in network size (from 400 to 2268 stations) and full driving range (from 353 to 388km).

Figure 12 plots (monetized) range anxiety against the full driving range of the EV observed in the data for 2021 and 2024 separately. There is strong negative relationship between range anxiety and the driving range of an EV. For an EV with a driving range of 200km in 2021, the lower end of the range distribution, range anxiety amounts to ¥44,000 (or 44% of the EV price), but range anxiety reduces to only ¥3000 for an EV with a driving range of 450km. The comparison between 2021 and 2024 shows range anxiety shifts down for an EV of the same range from 2021 to 2024 due to improvement in charging access.On average, range anxiety amounts to ¥13,600 ($1,900), or 10% of the EV price in 2021. In 2024, range anxiety drops to ¥8,400 ($1,200), or 4% of the EV price. The reduction was driven by both the increase in EV driving range (from 353km to 388km), and the charging station network size (from 400 to 2,268 stations), with the former contributing to 80% of the drop in range anxiety.

To further illustrate the role of charging access in affecting range anxiety, the two dotted

lines depict the level of range anxiety assuming the EV of a certain driving range only has the worst charging access (top) or the best charging access (bottom) observed in the data. Consistent with the intuition, charging access plays a bigger role for EVs with a low driving range. For EVs with a range of 200km, improving charging access from the worst to the best can reduce range anxiety from ¥46,000 to ¥30,000, a 35% reduction.

Figure A3 presents range anxiety with respect to driving range separately for two groups of EVs: those without access to home charging in panel (a), and those with access in panel (b). Panel (a) shows that range anxiety shifts down from 2021 to 2024 for an EV with the same driving range, due to the improvement in charging access. However, there is no visible shift in range anxiety from 2021 to 2024 for those with home chargers as shown in Panel (b), suggesting more limited role of access to public charging in addressing range anxiety for those with access to home charging. Comparing the two panels, average range anxiety does not differ significantly between these two groups of EVs due to a combination of two countervailing forces: (1) access to home charging relieves range anxiety; and (2) those with access to home charging tend to be less sensitive to charging price as the parameter estimates suggest.

5.3 Optimal Policy Design and Complementarity

In this section, I first discuss how the social value and cost of charging facilities and battery range are computed. Then I will conduct counterfactual analyses to (1) compute the optimal bundle of the two facilities in different years, and show that the current average range in 2024 is below optimal, while the number of stations has exceeded the optimal number. (2) show the complementarity of investing in both charming facility and battery range at the same time because of the diminishing return of each, highlighting the value of industry-public collaboration in promoting electric vehicles.

Back-of-Envelope Calculations on Value of Battery Capacity We evaluate the economic benefit of increasing driving range by adding battery capacity and compare it with the associated cost. To translate battery capacity (kWh) into driving range (km), we adopt a constant conversion factor of $\bar{E} = 6$ km/kWh.[9]

In addition, we assume a lifetime driving distance D (in km). Then the amount of electricity consumed per year is: $E = \frac{D}{\bar{E}}$. As a sanity check, a reasonable model should yield

[9]Other avenues to extend range— e.g., improvements in vehicle efficiency, aerodynamics, or thermal management— are outside the scope of this analysis; we hold them fixed and interpret the results as the value of additional battery capacity.

comparable orders of magnitude between the lifetime benefit of bigger battery and cost from a bigger battery. The cost is estimated to be roughly \$155 per kWh around 2021 and \$115 in 2024. Therefore, a 50 km increase in range would imply additional cost of $\frac{50 * \$115}{\bar{E}} =$ to $\frac{50 * \$155}{\bar{E}} =$ ¥6708 to 9042, which aligns well with the number of lifetime savings implied by the model in Figure 11.

Back-of-Envelope Calculations on Value of Network size We examine the economic benefit of adding an additional station to the Shanghai network. Each network will increase the average level of charging access with a diminishing return to scale. See Appendix Figure A4 for detailed relationship. At the station level d, the additional value of one station is given by $\frac{\partial CA}{\partial d}$. And we can evaluate the WTP for the station given by $\frac{\partial CA}{\partial d}\frac{\partial V(range,CA)}{\partial CA}$.

The social cost of a station is computed based on the industry report (need citation). Each charger costs about in 2018 to in 2024. We further assume 20 chargers per station and 1 million potential EV drivers as the population. We can evaluate the lifelong social cost of the station per consumer at. These two numbers guide us in designing the optimal number of charging stations for different types of consumers.

Trade-off Between Network size and Battery Range. To begin with, we solve the following optimization problem to get the optimal level of battery and network size at given social costs:

$$\max_{R,N} WTP(R,N) - \text{Battery Cost}(R) - \text{Charger Cost}(N) \tag{5}$$

Table 4 and Figure 13 report the optimal level, social welfare, and consumer WTP at the given level of a representative EV under the network in each given year.

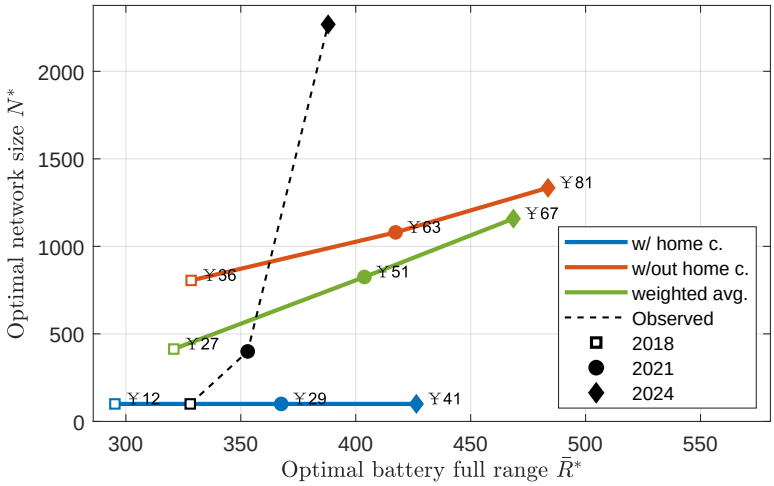
Complementarity in investing in battery and charging network Although battery capacity and charging-network size are strategic substitutes in the model— an arbitrarily large battery would eliminate the need for public charging, and an extremely dense network would offset limited range, fast diminishing returns to each technology imply that investing in both in a coordinated way is more effective than investing in just one. Figure A5 illustrates the intuition, and Table 5 empirically evaluates the optimal expansion path compared with the expansion path with focus on only one technology, and the observed expansion path, and shows which sector Shanghai is lagging in different years.

Table 4: Optimal Battery/Station Choices under Different Costs

Cost level	$\bar{R}_{\text{opt}}$ (km)	N_{opt}	Welfare	WTP	Cost
Panel A: w/ home c.					
2018	295	100	12.3	43.2	30.9
2021	368	100	29.3	60.5	31.1
2024	426	100	41.0	69.3	28.2
Panel B: w/out home c.					
2018	328	806	35.8	86.6	50.8
2021	417	1080	62.5	110.7	48.2
2024	484	1335	80.8	122.3	41.6
Panel C: weighted avg.					
2018	321	414	26.6	69.8	43.1
2021	404	825	50.7	94.3	43.6
2024	469	1158	67.3	106.1	38.8

Notes: Each panel corresponds to a consumer type. "Cost level" denotes the battery and station cost calculated for the year. We use grid search to find the optimal bundle $\{\bar{R} \in [250, 550], N \in [100, 2500]\}$. Welfare, WTP, and Cost are reported in thousands ¥, and are computed by comparing them with a car that has a full range of 200km and no fast-charging stations available.

Figure 13: Optimal levels of Battery Range and Charging Network Size



Notes: Each series traces the optimal pair $(\bar{R}^*, N^*)$—battery capacity (km) on the x-axis and charging-network size index on the y-axis—for three cost environments (2018, 2021, 2024). Blue: consumers *with* home chargers; orange: *without* home chargers; green: sample-weighted average (weights are the observed home-charger shares). The dashed black line connects the *observed* $(\bar{R}, N)$ in the data. Markers indicate years: □ 2018, • 2021, ◇ 2024. Currency labels next to the points report the model net surplus at the corresponding optimum (WTP minus cost, in 1,000 ¥). Connecting lines illustrate how optimal technology and infrastructure choices shift as battery and station costs change over time.

Table 5: Complementarity of Battery ($\bar{R}$) and Network Size (N)

Scenario	$\bar{R}$ (km)	N	Welfare	WTP	Cost
Panel A: 2018 level of battery and station cost					
A: $(\bar{R}^{opt}, N^{opt})$	321	414	26.6	69.8	43.1
B: $(\bar{R}^{obs}, N^{obs})$	318	100	22.5	60.4	38.0
C: $(\bar{R}^{opt}, N^{obs})$	327	100	22.5	63.3	40.7
D: $(\bar{R}^{obs}, N^{opt})$	318	414	26.6	68.9	42.2
Panel B: 2021 level of battery and station cost					
A: $(\bar{R}^{opt}, N^{opt})$	404	825	50.7	94.3	43.6
B: $(\bar{R}^{obs}, N^{obs})$	353	400	47.7	78.7	30.9
C: $(\bar{R}^{opt}, N^{obs})$	411	400	49.7	91.2	41.5
D: $(\bar{R}^{obs}, N^{opt})$	353	884	49.1	84.0	34.9
Panel C: 2024 level of battery and station cost					
A: $(\bar{R}^{opt}, N^{opt})$	469	1158	67.3	106.1	38.8
B: $(\bar{R}^{obs}, N^{obs})$	388	2268	62.7	97.3	34.6
C: $(\bar{R}^{opt}, N^{obs})$	461	2268	64.9	108.4	43.5
D: $(\bar{R}^{obs}, N^{opt})$	388	1315	64.7	94.4	29.7

Notes: Each panel corresponds to cost levels in the indicated year. $(\bar{R}^{opt}, N^{opt})$ denotes the welfare-maximizing pair, $(\bar{R}^{obs}, N^{obs})$ fixes both at observed levels in each year, and mixed cases optimize only one dimension while holding the other fixed at observed. The welfare number is computed by comparing it with a car that has a full range of 200km and no fast-charging stations available.

6 Conclusion

Although range anxiety consistently emerges as a key barrier to EV adoption in consumer surveys, industry reports, and policy discussions, there has been little economic analysis quantifying its magnitude and evaluating the effectiveness of potential remedies. To our knowledge, this study is the first to micro-found range anxiety, the utility loss from unrealized but feasible trips due to fear of depleting power before reaching a charging station, within a continuous-time dynamic model of EV driving and charging behavior. Using high-frequency usage and charging data from 8,000 EVs in Shanghai, we estimate average range anxiety at \$1,900 in 2021, declining to \$1,200 in 2024. This decline is primarily driven by the expansion of the charging network (from 400 to 2,268 stations) and, especially, by improvements in EV driving range (from 353 km to 388 km) over this period.

Our simulations highlight the crucial roles of two approaches in addressing range anxiety: expanding driving range (through increased battery capacity) and enhancing charging access (through larger charging networks). Because each approach exhibits diminishing returns, the welfare-maximizing policy requires coordinated investment in both charging infrastructure and battery capacity. The socially optimal levels of charging network size and driving range

evolve as the costs of charging-station construction and battery production decline over time. Our analysis indicates that the realized investment trajectory diverges significantly from the optimal path: by 2024, Shanghai has over-invested in charging infrastructure while under-investing in driving range relative to the social optimum.

We note two important caveats and directions for future research. First, our data and analysis are restricted to travel within Shanghai, and thus our estimates of range anxiety likely represent a lower bound, as range anxiety may be more pronounced for long-distance trips. That said, long-distance driving is less common in China than in countries such as the U.S., partly due to China's extensive high-speed rail system. Second, our empirical analysis is based on data from Shanghai, and the quantitative findings should be interpreted in that context. As detailed EV usage and charging data become available elsewhere, our framework can be adapted to quantify range anxiety and its policy implications across different settings, where underlying preferences may vary. Another important direction for future research is to leverage granular data to examine the optimal spatial distribution of charging infrastructure.

References

Arkolakis, Costas, Kenneth T. Gillingham, and Seung-Yong Yoo, "Optimizing Electric Vehicle Infrastructure," *AEA Papers and Proceedings*, May 2025, *115*, 563–67.

Bailey, Megan R., David P. Brown, Blake C. Shaffer, and Frank A. Wolak, "Show Me the Money! A Field Experiment on Electric Vehicle Charge Timing," *American Economic Journal: Economic Policy*, 2025, *17* (2), 259–284.

Barwick, Panle Jia, Christopher Knittel, Shanjun Li, Youming Liu, James Stock, and Binglin Wang, "Optimal Charging Infrastructure for Electric Vehicles," Working Paper 2025.

_ , Hyuk-Soo Kwon, and Shanjun Li, "Attribute-based Subsidies and Market Power: an Application to Electric Vehicles," Working Paper 32264, National Bureau of Economic Research March 2024.

Bernard, Louise, Andy Hackett, Robert Metcalfe, Luca Panzone, and Andrew Schein, "The Impact of Dynamic Prices on Electric Vehicle Public Charging Demand: Evidence from a Nationwide Natural Field Experiment," Technical Report, Centre for Net Zero May 2025. Working Paper.

Bloomberg Intelligence, "Global Battery Electric Vehicle Outlook," 2024.

Burlig, Fiona, James Bushnell, David Rapson, and Catherine Wolfram, "Low Energy: Estimating Electric Vehicle Electricity Use," *AEA Papers and Proceedings*, May 2021, *111*, 430–35.

Chokshi, Niraj, Matthew Goldstein, and Erin Woo, "Biden's electric car plans hinge on having enough chargers," *The New York Times*, 2021. Accessed: 2025-07-12.

Dorsey, Jackson, Ashley Langer, and Shaun McRae, "Fueling alternatives: Gas station choice and the implications for electric charging," *American Economic Journal: Economic Policy*, 2025, *17* (1), 362–400.

Garg, Teevrat, Ryan Hanna, Jeffrey Myers, Sebastian Tebbe, and David G. Victor, "Electric Vehicle Charging at the Workplace: Experimental Evidence on Incentives and Environmental Nudges," CESifo Working Paper 11445, CESifo, Munich 2024.

Heid, Pascal, Kevin Remmy, and Mathias Reynaert, "Equilibrium Effects in Complementary Markets: Electric Vehicle Adoption and Electricity Pricing," *TSE Working Paper*, 2024.

Jacqz, Irene and Sarah Johnston, "Electric Vehicle Subsidies and Urban Air Pollution Disparities," *Journal of the Association of Environmental and Resource Economists*, 2024, *11* (S1).

Klier, Thomas H. and James M. Rubenstein, "North America's Rapidly Growing Electric Vehicle Market: Implications for the Geography of Automotive Production," *Economic Perspectives*, December 2022, *No. 5.* Accessed: 2025-07-12.

La Nauze, Andrea, Lana Friesen, Kai Li Lim, Flavio M. Menezes, Lionel Page, Thara Philip, and Jake Whitehead, "Can Electric Vehicles Aid the Renewable Transition? Evidence from a Field Experiment Incentivising Midday Charging," CESifo Working Paper 11386, CESifo, Munich 2024.

Li, Jing, "Compatibility and investment in the us electric vehicle market," *Unpublished manuscript, MIT*, 2023.

Li, Shanjun, Lang Tong, Jianwei Xing, and Yiyi Zhou, "The market for electric vehicles: indirect network effects and policy design," *Journal of the Association of Environmental and Resource Economists*, 2017, *4* (1), 89–133.

Liu, Zikun, "Policy Design for Sustainable Innovation and Adoption: A Structural Analysis of the Electric Vehicle Market," 2025. Working Paper.

Qin, Molin and Jonathan Scott, "The High Cost of Low Range: Estimating the Hidden Cost of Range Anxiety in Electric Vehicles," *Working Paper*, 2023.

Rainieri, Giuseppe, Chiara Buizza, and Alberto Ghilardi, "The psychological, human factors and socio-technical contribution: A systematic review towards range anxiety of battery electric vehicles' drivers," *Transportation Research Part F: Traffic Psychology and Behaviour*, 2023, *99*, 52–70.

Rapson, David S. and Erich Muehlegger, "The economics of electric vehicles," *Review of Environmental Economics and Policy*, 2023, *17* (2), 274–294.

Remmy, Kevin, "Adjustable Product Attributes, Indirect Network Effects, and Subsidy Design: The Case of Electric Vehicles," 2025. Working Paper.

Springel, Katalin, "It's Not Easy Being "Green": Lessons from Norway's Experience with Incentives for Electric Vehicle Infrastructure," *Review of Environmental Economics and Policy*, 2021, *15* (2).

_ , "Network externality and subsidy structure in two-sided markets: Evidence from electric vehicle incentives," *American Economic Journal: Economic Policy*, 2021, *13* (4), 393–432.

Wang, Yucheng, "Who Receives Environmental Benefits from Driving Electric Vehicles?," *Unpublished Manuscript*, April 2024.

Wardlaw, Christian, "What is Range Anxiety with Electric Vehicles?," J.D. Power November 2020. Accessed 2025-07-12.

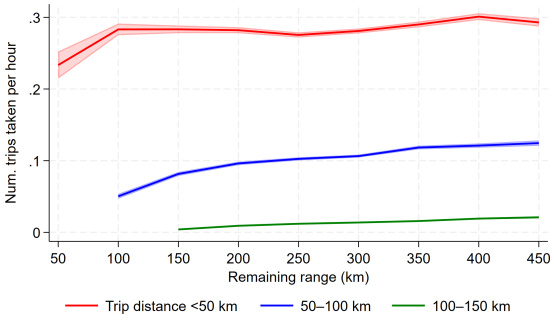
Zhou, Yiyi and Shanjun Li, "Technology Adoption and Critical Mass: The Case of the U.S. Electric Vehicle Market," *The Journal of Industrial Economics*, 2018, *66* (2), 423–480.

Online Appendix

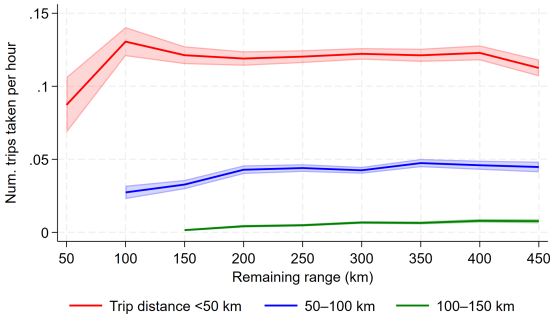
A Appendix Figures

Figure A1: Observed Trip Hazard Rates by Remaining Range

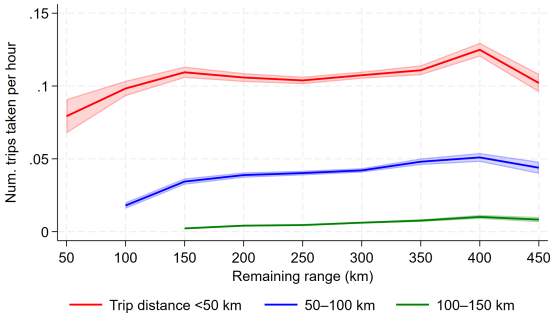
(a) Morning time only



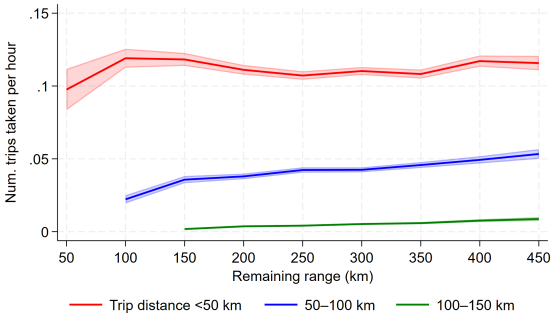
(b) Weekend time only



(c) Winter time only



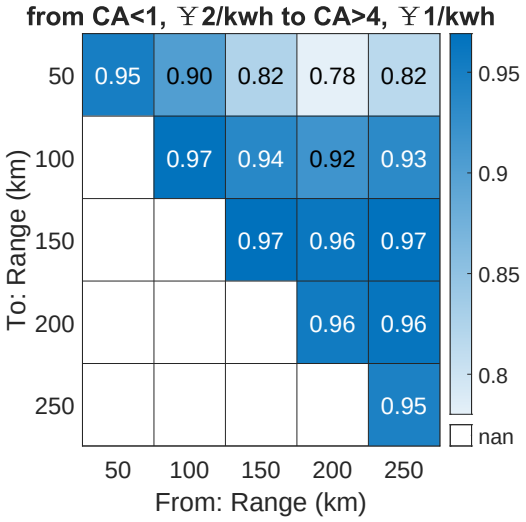
(c) Summer time only



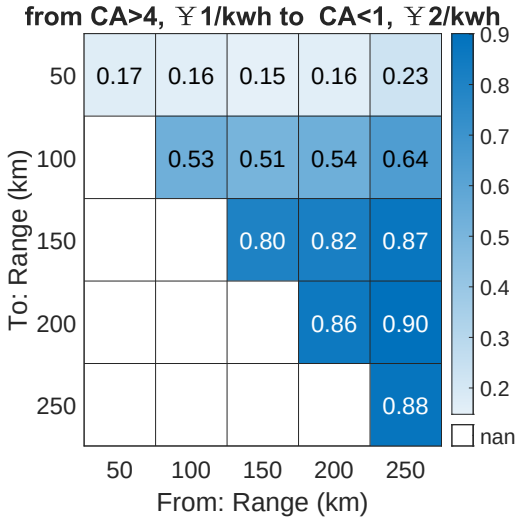
Notes: Each colored line corresponds to a trip with a certain distance: $<$ 50 km, 50–100 km, 100–150 km, and 150–200 km. Hazard rates by the y-axis are computed as the number of trips initiated per hour from each starting remaining range (x-axis), normalized by the hours vehicles stay in that state (until a trip arrives). Shaded areas show 95% confidence intervals. Each panel presents the results for a specific time frame. The overall pattern is consistent with that from pooling all the data together.

Figure A2: Estimated Trip-taking policy function $h^{H=0,\bar{R}=500}(b, r, p)$

(a) Travelling policy



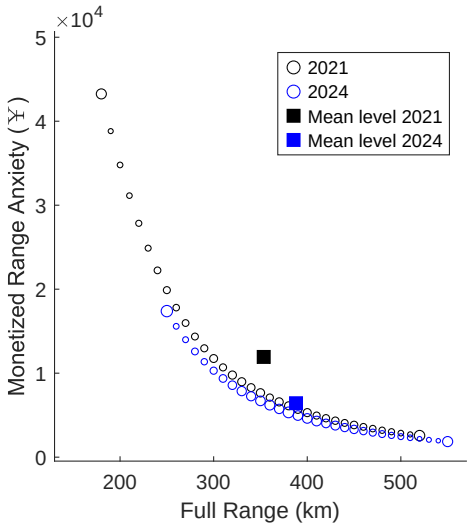
(b) Travelling policy



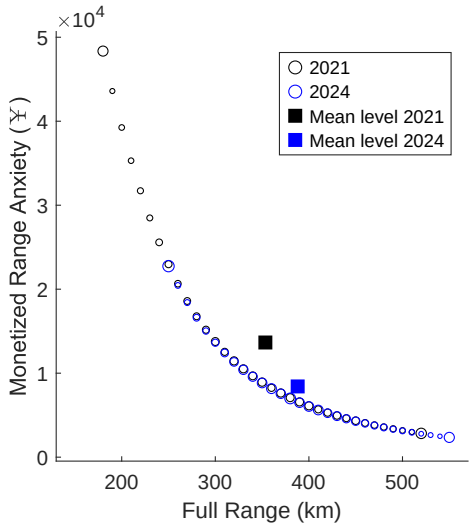
Notes: This figure presents the estimated policy functions governing charging and traveling decisions. Panels (a) and (b) display the probability of taking a trip with a starting range (x-axis) to an end range (y-axis). "Nan" denotes infeasible trips. Darker shades represent higher probabilities. Each heatmap cell corresponds to the probability of taking the trip that moves the car from a given initial range (x-axis) to a new remaining range (y-axis).

Figure A3: Range Anxiety by Access to Home Charging

(a) Range anxiety w/o home chargers

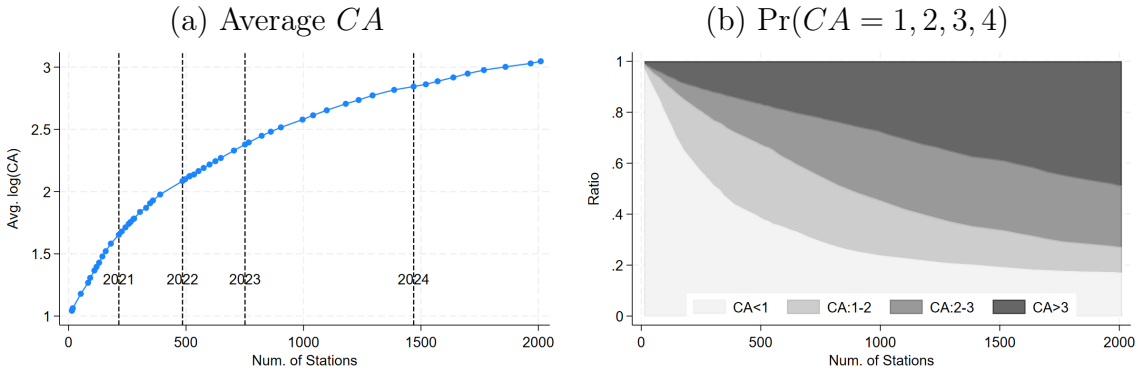


(b) Range anxiety with home chargers



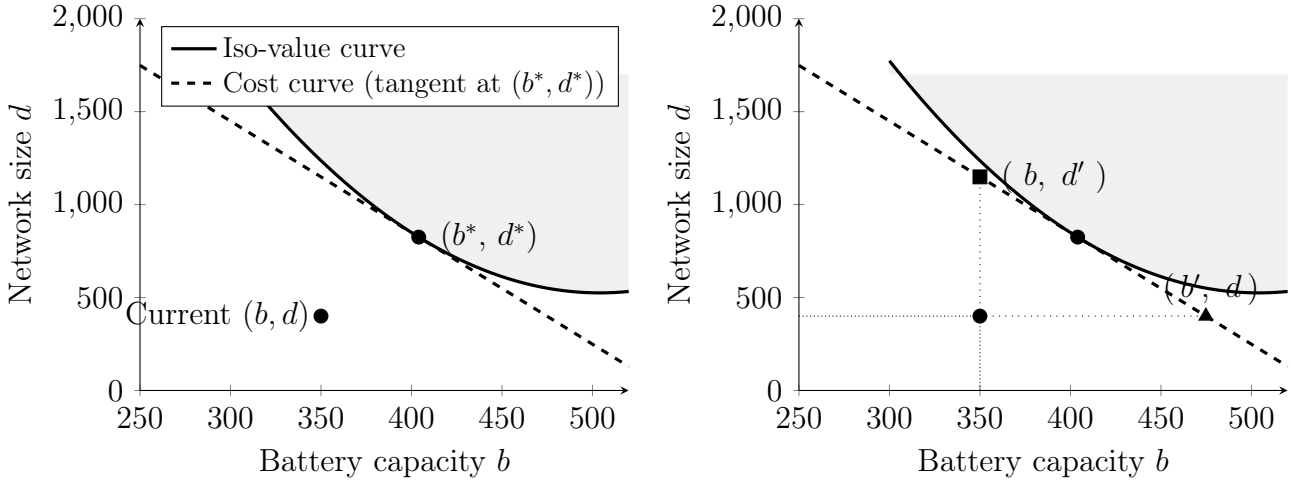
Notes: Each panel plots *monetized range anxiety* (lifetime WTP, 10^4 ¥) against the vehicle's full range (km). Circle area is proportional to the empirical frequency of each full-range level in that year's sample. Filled squares mark the weighted mean level for the year. Panel (a) evaluates consumers *without* home charging; panel (b) evaluates consumers *with* home charging. The downward slope indicates that range anxiety declines with battery range; the downward shift from 2021 to 2024 reflects improvements in network size and prices.

Figure A4: Relationship between charging access and number of stations



Notes: Charging access (CA) is an inverse–distance–squared index for each location i, $\text{CA}_i = \sum_j 1/\text{dist}_{ij}^2$, where nearby stations receive more weight. **Panel (a)** plots the sample average of log(CA) as the total number of stations increases; the vertical dashed lines mark the observed station counts in 2021–2024. The concavity indicates diminishing marginal improvements in access as the network grows. **Panel (b)** shows how the cross-sectional distribution of access shifts with network size: stacked areas are the shares of locations falling in four CA bins (< 1, 1–2, 2–3, > 3).

Figure A5: Policy coordination between battery capacity and network density.



(a) Iso-value (solid) and cost (dashed); optimum at tangency.

(b) One-dimensional moves along the cost line: improve only d (to d') or only b (to b').

Notes: The figure illustrates **policy coordination** between battery capacity b and charging-network size d. The solid curve is an iso-value (welfare) contour: combinations above the curve (light shading) deliver higher welfare. The dashed line is the *cost* trade-off—here drawn as the tangent at the optimum (b^*, d^*)—representing budgets or relative prices that keep total cost constant along the line. **Panel (a)** shows the optimum at the tangency of the iso-value and cost curves; the current configuration (b, d) lies below that level set. **Panel (b)** decomposes incremental policies from the current point: moving vertically to (b, d') improves only network size, while moving horizontally to (b', d) improves only battery capacity, both along the same cost line. Because b and d exhibit diminishing marginal returns, coordinated investments that move (b, d) toward the tangency typically achieve larger welfare gains than one-sided changes that adjust only b or only d.

B Appendix Tables

Table A1: Dataset Overview

Year	2021				2024			
	Winter	Spring	Summer	Fall	Winter	Spring	Summer	Fall
Driver info								
# Drivers	1100	1100	1100	1100	1100	1100	1100	1100
Avg. range (km)	293	357	356	381	332	411	378	416
With home charger	75.1%	61.9%	62.8%	57.2%	67.0%	64.8%	66.7%	63.5%
Driving Trips per driver per week								
Count	20.9	20.3	20.5	20.9	23.4	21.6	21.7	21.7
Total distance (km)	376.4	388.5	381.8	405.6	477.2	447.1	447.6	514
Total duration (hour)	15.6	16.3	15.8	16.1	19.2	18.4	18.8	19
Chargings per driver per week								
# Fast	0.7	0.9	0.9	1.1	1.5	1.2	1.3	1.1
# Slow	2.5	1.9	1.9	1.6	3.5	2.4	2.6	2.1
Fast Duration (hour)	2.3	1.6	1.7	1.9	2.1	1.8	1.8	1.7
Slow Duration (hour)	14.7	13	13.3	11.7	13.6	11	12.4	12.2
Fast Starting SOC	35	37	34	33	40	44	39	39
Slow Starting SOC	47	48	45	45	49	50	46	45

Note: The dataset in each year includes four weekly cross-sections of 1100 randomly selected EVs from the EV stock in Shanghai during Jan 23-30 (Winter), March 20-27 (Spring), Aug 23-30 (Summer), and Oct 20-27 (Fall). In total, there are 188,707 driving trips, about 16,986 slow charging sessions, and about 8,524 fast charging sessions. Driving range is calculated based on the data: $\frac{\text{Total distance driven}}{\text{Total battery consumed}} \times \text{Battery Size}$.